

AD 745214

AD

USAAMRDL TECHNICAL REPORT 72-22

INVESTIGATION OF THE SPEED BRAKES ON THE S-67 AIRCRAFT

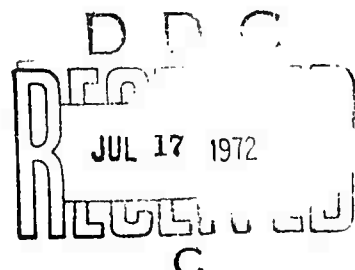
By

N. F. K. Kefford

May 1972

EUSTIS DIRECTORATE
U. S. ARMY AIR MOBILITY RESEARCH AND DEVELOPMENT LABORATORY
FORT EUSTIS, VIRGINIA

CONTRACT DAAJ02-71-C-0009
UNITED AIRCRAFT CORPORATION
SIKORSKY AIRCRAFT DIVISION
STRATFORD, CONNECTICUT

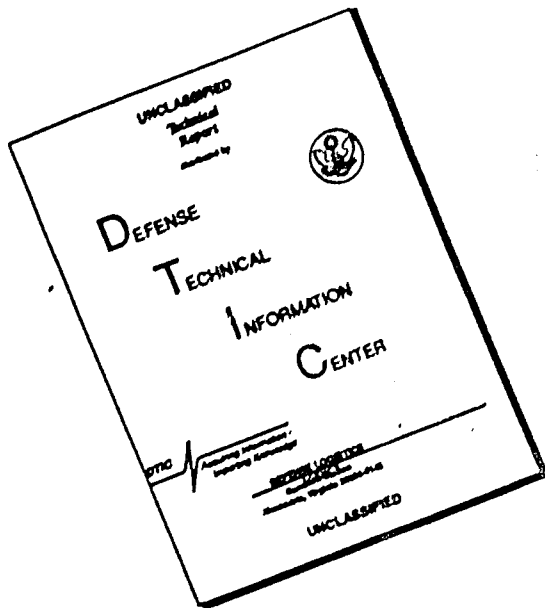


Approved for public release;
distribution unlimited.



Reproduced by
NATIONAL TECHNICAL
INFORMATION SERVICE
U.S. Department of Commerce
Springfield VA 22151

DISCLAIMER NOTICE



**THIS DOCUMENT IS BEST
QUALITY AVAILABLE. THE COPY
FURNISHED TO DTIC CONTAINED
A SIGNIFICANT NUMBER OF
PAGES WHICH DO NOT
REPRODUCE LEGIBLY.**

DISCLAIMERS

The findings in this report are not to be construed as an official Department of the Army position unless so designated by other authorized documents.

When Government drawings, specifications, or other data are used for any purpose other than in connection with a definitely related Government procurement operation, the United States Government thereby incurs no responsibility nor any obligation whatsoever; and the fact that the Government may have formulated, furnished, or in any way supplied the said drawings, specifications, or other data is not to be regarded by implication or otherwise as in any manner licensing the holder or any other person or corporation, or conveying any rights or permission, to manufacture, use, or sell any patented invention that may in any way be related thereto.

Trade names cited in this report do not constitute an official endorsement or approval of the use of such commercial hardware or software.

DISPOSITION INSTRUCTIONS

Destroy this report when no longer needed. Do not return it to the originator.

ACCESSION for	
CFSTI	WHITE SECTION <input checked="" type="checkbox"/>
DDC	BUFF SECTION <input type="checkbox"/>
ANNOUNCED <input type="checkbox"/>	
JUSTIFICATION	
.....	
BY	
DISTRIBUTION/AVAILABILITY CODES	
DIST.	AVAIL. and/or SPECIAL
A	

Unclassified

Security Classification

DOCUMENT CONTROL DATA - R & D

(Security classification of title, body of abstract and indexing annotation must be entered when the overall report is classified)

1. ORIGINATING ACTIVITY (Corporate author) Sikorsky Aircraft Division United Aircraft Corporation Stratford, Connecticut		2a. REPORT SECURITY CLASSIFICATION Unclassified 2b. GROUP	
3. REPORT TITLE INVESTIGATION OF THE SPEED BRAKES ON THE S-67 AIRCRAFT			
4. DESCRIPTIVE NOTES (Type of report and inclusive dates) Final Report			
5. AUTHOR(S) (First name, middle initial, last name) N.F.K. Kefford			
6. REPORT DATE April 1972	7a. TOTAL NO. OF PAGES 57	7b. NO. OF REFS 4	
8a. CONTRACT OR GRANT NO. DAAJ02-71-C-0009	9a. ORIGINATOR'S REPORT NUMBER(S) USAAMRDL Technical Report 72-22		
b. PROJECT NO.			
c. Task 1F163204D15704	9b. OTHER REPORT NO(S) (Any other numbers that may be assigned this report) SER-67007		
d.			
10. DISTRIBUTION STATEMENT Approved for public release; distribution unlimited.			
11. SUPPLEMENTARY NOTES	12. SPONSORING MILITARY ACTIVITY Eustis Directorate U.S. Army Air Mobility R&D Laboratory Fort Eustis, Virginia		
13. ABSTRACT Under Contract DAAJ02-71-C-0009, Sikorsky Aircraft conducted flight tests and computer simulations to evaluate speed brakes for a winged helicopter. The flight test program established the effectiveness of wing-mounted speed brakes for increasing dive angle, deceleration capability, and maneuverability of the Sikorsky S-67. In the configuration tested, six brake surfaces operated together to increase aircraft drag by 155% while reducing wing lift. With these speed brakes, dive angles could be increased from 5 to 7 degrees at 140 knots dependent upon the initial dive angle. At 160 knots, the increase in dive angle varies from 8 to 9 degrees. These increases in aircraft dive angle due to speed brake extension can be further increased by allowing the aircraft to accelerate during the dive. Dive characteristics with and without speed brakes extended were obtained. A dive envelope defined by control and airframe stress limits was established that provided a broad dive envelope of forward speed and collective settings to achieve various dive angles. Above dive speeds of 120 knots, the brakes caused a decrease in fuselage attitude to the flight path of 4 to 5 degrees, for a given dive angle. This, coupled with the steeper dive angles, improves the aircraft's capability as a weapons platform. Speed brakes enabled constant-altitude deceleration from 180 to 140 knots in 9 seconds as compared to 24 seconds with a clean wing. The computer simulation program examined increased brake area, variable stabilator bias angle, and the consequences of asymmetric brake deployment. Steady dive angles of 30 degrees or more were possible with increased brake area. Following any configuration of asymmetric brake deployment, there was always sufficient roll control power to restore and hold trim, although some deceleration occurred due to collective and/or power limits.			

DD FORM 1 NOV 1973

REPLACES DD FORM 1473, 1 JAN 64, WHICH IS
OBSOLETE FOR ARMY USE.

Unclassified

Security Classification

Unclassified

Security Classification

14 KEY WORDS	LINK A		LINK B		LINK C	
	ROLE	WT	ROLE	WT	ROLE	WT
Helicopter Winged Helicopter Sikorsky S-67 Aerodynamics Dive Deceleration Maneuverability Speed Brakes						

Unclassified

Security Classification

11a



DEPARTMENT OF THE ARMY
U. S. ARMY AIR MOBILITY RESEARCH & DEVELOPMENT LABORATORY
EUSTIS DIRECTORATE
FORT EUSTIS, VIRGINIA 23604

This report was prepared by United Aircraft Corporation, Sikorsky Aircraft Division, under Contract DAAJ02-71-C-0009.

The program was a flight investigation of wing-mounted speed brakes as installed on the S-67 winged helicopter. A computer simulation study was included to determine the effects of increased brake area, variable stabilator bias angle, and asymmetric brake deployment. This program is one of four flight investigations conducted on the S-67 winged helicopter. The other three flight investigations were concerned with a stabilator, a force-feel control system, and aircraft maneuverability.

The wing-mounted speed brakes on the S-67 aircraft increase the dive angle and reduce the fuselage attitude relative to the flight path. At 140 knots airspeed, the increase in dive angle varies from 5 to 7 degrees dependent upon the initial dive angle. At 160 knots, the increase in dive angle varies from 8 to 9 degrees. The aircraft dive angle may be further increased by allowing the aircraft to accelerate during the dive. The amount of reduction in fuselage angle relative to the flight path varies from 4 to 5 degrees for all airspeeds above 120 knots. The speed brakes enable the S-67 aircraft to be decelerated in level flight from 180 to 140 knots in 9 seconds as compared to 24 seconds without the use of brakes.

The report has been reviewed by this Directorate and is technically correct.

This program was conducted under the technical management of Mr. R. C. Dumond of the Applied Aeronautics Division.

11b
oo

Task 1F163204D15704
Contract DAAJ02-71-C-0009
USAAMRDL Technical Report 72-22
May 1972

INVESTIGATION OF THE SPEED BRAKES ON
THE S-67 AIRCRAFT

SER-67007

by

N. F. K. Kefford

Prepared by

United Aircraft Corporation
Sikorsky Aircraft Division
Stratford, Connecticut

for

EUSTIS DIRECTORATE
U. S. ARMY AIR MOBILITY RESEARCH AND DEVELOPMENT LABORATORY
FORT EUSTIS, VIRGINIA

Approved for public release;
distribution unlimited.

11C

ABSTRACT

Under Contract DAAJ02-71-C-0009, Sikorsky Aircraft conducted flight tests and computer simulations to evaluate speed brakes for a winged helicopter.

The flight test program established the effectiveness of wing-mounted speed brakes for increasing dive angle, deceleration capability, and maneuverability of the Sikorsky S-67. In the configuration tested, six brake surfaces operated together to increase aircraft drag by 155% while reducing wing lift. With these speed brakes, dive angles could be increased from 5 to 7 degrees at 140 knots dependent upon the initial dive angle. At 160 knots, the increase in dive angle varies from 8 to 9 degrees. These increases in aircraft dive angle due to speed brake extension can be further increased by allowing the aircraft to accelerate during the dive.

Dive characteristics with and without speed brakes extended were obtained. A dive envelope defined by control and airframe stress limits was established that provided a broad dive envelope of forward speed and collective settings to achieve various dive angles.

Above dive speeds of 120 knots, the brakes caused a decrease in fuselage attitude to the flight path of 4 to 5 degrees, for a given dive angle. This, coupled with the steeper dive angles, improves the aircraft's capability as a weapons platform.

Speed brakes enabled constant-altitude deceleration from 180 to 140 knots in 9 seconds as compared to 24 seconds with a clean wing.

The computer simulation program examined increased brake area, variable stabilator bias angle, and the consequences of asymmetric brake deployment. Steady dive angles of 30 degrees or more were possible with increased brake area. Following any configuration of asymmetric brake deployment, there was always sufficient roll control power to restore and hold trim, although some deceleration occurred due to collective and/or power limits.

FOREWORD

This report presents results of flight tests and computer simulations to investigate the effectiveness of speed brakes for increasing dive angle, deceleration capability, and maneuverability of the S-67 aircraft. This program is part of a four-phase investigation of the flight characteristics of the S-67 aircraft as a representative high-speed winged helicopter. Investigations of the stabilator, aircraft maneuverability, and a Feel Augmentation System (FAS) are also part of the flight investigation of the S-67. The FAS is a system to provide "force-feel" in pitch.

The work was performed by the Sikorsky Aircraft Division of United Aircraft Corporation for the U.S. Army Air Mobility Research and Development Laboratory, Fort Eustis, Virginia, under Contract DMA02-71-C-0009, DA Task 1F163204D15704. Mr. R. C. Dumond was the Army technical representative.

Preceding page blank

TABLE OF CONTENTS

	Page
ABSTRACT	iii
FOREWORD	v
LIST OF ILLUSTRATIONS	viii
LIST OF SYMBOLS	x
INTRODUCTION	1
DESCRIPTION OF AIRCRAFT	2
THE S-67 SPEED BRAKES	6
FLIGHT TEST CONDITIONS	7
Loading	7
Flight	7
Stabilator Bias Angle	7
RESULTS AND DISCUSSION	8
Level Flight.	8
Dive Angle and Fuselage Angle of Attack	8
Dive Envelope	9
Maximum Engine Torque Limit	10
Minimum Engine Torque Limit	10
Main Rotor Control Loads	10
Stabilator Vibratory Stress	10
Lack of Right Pedal Control	11
Speed Brake Extension and Retraction, Controls Fixed	11
Decelerations and Turns	11
Computer Simulation Study	12
Increased Brake Effectiveness	12
Effect of Stabilator Bias Angle	12
Asymmetric Deployment	13
CONCLUSIONS	14
LITERATURE CITED	15
APPENDIXES	
I. S-67 Wind Tunnel Data	39
II. Computer Simulation Study	41
DISTRIBUTION	48

LIST OF ILLUSTRATIONS

<u>Figure</u>		<u>Page</u>
1	The S-67 Aircraft, Quarter View	16
2	Speed Brake Areas and Locations	17
3	In-Flight Front View, Speed Brakes Retracted	18
4	In-Flight Front View, Speed Brakes Extended	18
5	Speed Brake Controls	19
6	Trim Level-Flight Characteristics, GW = 17,300 lb, cg = 258 in..	20
7	Trim Level-Flight Characteristics, GW = 14,800 lb, cg = 276 in.	21
8	Trim Level-Flight Characteristics, GW = 17,300 lb, cg = 276 in	22
9	Dive Characteristics, GW = 14,800 lb, cg = 276 in., Speed Brakes Extended	23
10	Dive Characteristics, GW = 17,300 lb, cg = 276 in., Speed Brakes Retracted	24
11	Dive Characteristics, GW = 17,300 lb, cg = 276 in., Speed Brakes Extended	25
12	Fuselage Angle of Attack, GW = 17,300 lb, cg = 276 in., V = 140 kt.	26
13	Fuselage Angle of Attack vs. Engine Torque and Forward Speed, GW = 17,300 lb, cg = 276 in., Speed Brakes Extended	27
14	Simulation of Dive Characteristics, Speed Brakes Retracted, GW = 14,800 lb, cg = 276 in.	28
15	Simulation of Dive Characteristics, Speed Brakes Extended, GW = 14,800 lb, cg = 276 in.	29
16	Collective vs. Engine Torque, GW = 17,300 lb, cg = 276 in..	30
17	Dive Angle vs. Engine Torque and Forward Speed, GW = 17,300 lb, cg = 276 in., Speed Brakes Extended	31
18	Tail Rotor Pitch vs. Engine Torque and Forward Speed, GW = 17,300 lb, cg = 276 in., Speed Brakes Extended	32

<u>Figure</u>	<u>Page</u>
19 Transient Effects of Speed Brake Extension at $V = 180$ kt, Controls Fixed	33
20 Deceleration From $V = 180$ to $V = 140$ kt, Without Speed Brakes	34
21 Deceleration From $V = 180$ to $V = 140$ kt, With Speed Brakes	35
22 Simulation of Dive Characteristics, Speed Brake Extended, $GW = 14,800$ lb, $cg = 276$ in., Double Existing Brake Area .	36
23 Simulation of Dive Characteristics, Speed Brakes Extended, $GW = 14,800$ lb, $cg = 276$ in., Stabilator Bias Angle = 5.0 deg	37
24 Speed Brake Panel Identification	38
25 S-67 Wind Tunnel Data, Showing Lift, Pitching Moment, and Drag vs. Fuselage Angle of Attack for Total Aircraft Less Wings, With Wings, and Speed Brakes Retracted and Extended	40
26 Comparison Between Simulated and Flight Test Data, Level Flight Trim, $GW = 14,800$ lb, $cg = 276$ in., Stabilator Bias = 0 deg, Speed Brakes Retracted	43
27 Comparison Between Simulated and Flight Test Data, Level Flight Trim, $GW = 14,500$ lb, $cg = 275$ in., Stabilator Bias = 0 deg, Speed Brakes Extended	45
28 Comparison Between Simulated and Flight Test Data, Level Flight Trim, $GW = 16,800$ lb, $cg = 258$ in., Stabilator Bias = 2.5 deg, Speed Brakes Extended.	46
29 Comparison Between Simulated and Flight Test Data, Level Flight Trim, $GW = 17,200$ lb, $cg = 275$ in., Stabilator Bias = 2.5 deg, Speed Brakes Extended	47

LST OF SYMBOLS

A_1 _s	lateral cyclic control, %
B_1 _s	longitudinal cyclic control, %
i_t	stabilator incidence angle, deg
N_R	main rotor speed, rpm
$\dot{\tau}_E$	required engine torque, %
RCD	rate of descent, fpm
τ_E	required shaft horsepower, hp
V_f	forward speed, kt
V_{fmax}	maximum level-flight forward speed, kt
α	fuselage angle of attack, deg
β	fuselage sideslip angle, deg
γ	dive angle, deg
θ_{TR}	tail rotor blade pitch, deg
θ_F	fuselage pitch attitude, deg
θ_O	main rotor collective control, %
θ_{cuff}	main rotor collective blade pitch, deg
ϕ_F	fuselage roll attitude, deg

INTRODUCTION

Experience with high-performance helicopters has indicated that aerodynamic speed brakes would improve control characteristics and maneuverability. They should reduce aircraft acceleration in a dive as well as reduce wing lift. This would permit steeper dives and rapid decelerations.

Wind tunnel testing of the aerodynamic effects of speed brakes resulted in the present arrangement of six unperforated panels mounted on the wings of the S-67 aircraft.

The speed brakes on the S-67 aircraft were evaluated in flight tests to determine their effectiveness for increasing dive angle, deceleration capability and maneuverability on a high-speed winged helicopter. The test results were correlated with a computer simulation study, and the simulation was used to predict the effects of different brake areas, stabilator bias angle and asymmetric brake deployment.

DESCRIPTION OF AIRCRAFT

The S-67 demonstrator is a high-speed derivative of the Sikorsky SH-3D helicopter. A view of the aircraft is presented in Figure 1. The low-drag airframe was designed to meet requirements of an attack mission. The cockpit is arranged in tandem, with the gunner in the forward seat and the pilot in the aft, elevated seat. The pilot has visibility down to minus 15 degrees and the gunner has visibility up to plus 15 degrees. Both seats are mounted in a seat mount system above the fuselage center section.

Main rotor hub, tail rotor, drive system, and transmission systems are all SH-3D dynamic components. The main rotor has five S-61F blades, each with a twist of -4 degrees. The 22-inch blade tips are swept back 20 degrees to delay tip Mach number effects. The control system uses SH-3D components and the CH-54 automatic flight control system.

The fixed-wing type control surfaces include a stabilator, a fixed vertical stabilizer, and sponsons with stub wings for additional lift. The tail wheel is attached to the base of the ventral fin, and the retractable main landing gear is housed in the wing. The wing panels have speed brakes to control dive angle and increase deceleration capability. Flight control sensitivities are listed in the table below.

FLIGHT CONTROL SENSITIVITIES

	Servo Travel per Inch (%)	Blade Pitch per Inch (%)	Stick/Pedal Travel (in.)	Blade Pitch Travel (deg)
Longitudinal Cyclic	7.2	1.7	14	24
Lateral Cyclic	7.2	1.4	14	16
Pedals	24.6*	7.75 (Tail Rotor)	4.07*	31.5 (Tail Rotor)
Collective	10.5	1.7	9.5	16

* Working range, at constant collective

Principal dimensions and general data for the S-67 aircraft are as follows:

Main Rotor

Diameter	62 ft
Normal Tip Speed ($10^4 \%$ N_R)	686 ft/sec
Disc Area	3019 ft^2
Solidity	0.0781
Number of Blades	5
Blade Chord	1.52 ft
Blade Twist	-4 deg
Airfoil Section	NACA 0012 MOD
Articulation	Full Flapping and Lagging
Tip Sweep	20 deg

Tail Rotor

Diameter	10 ft 4 in.*
Tip Speed	700 ft/sec
Disc Area	83.9 ft^2
Solidity	0.1885
Number of Blades	5
Blade Chord	0.612 ft
Blade Twist	0 deg
Airfoil Section	NACA 0012 MOD
Pitch Flap Coupling	45 deg

* During flight tests, diameter was increased 3 in. to 10 ft. 7 in. to increase lateral low-speed flight capability.

Fuselage

Overall Length	64 ft 1 in.
Overall Height	16 ft 3 in.
Overall Width	27 ft 4 in.
Wheel Tread	7 ft
Wheel Base	36 ft 2 in.

Stabilator

Root Chord	4 ft 2 in.
Tip Chord	2 ft
Taper Ratio	0.48
Area	50 ft ²
Span	15 ft 6 in.
Aspect Ratio	4.8
Airfoil (Root)	NACA 0015
Airfoil (Tip)	NACA 0012

Vertical Fin

Root Chord	7 ft 6 in.
Tip Chord (Upper)	2 ft 10 in.
Tip Chord (Lower)	3 ft 9 in.
Taper Ratio (Upper)	0.62
Taper Ratio (Lower)	0.5
Total Area	68.7 ft ²
Aspect Ratio	2.65
Airfoil Section	NACA 4415

Wing

Root Chord	4 ft 6 in.
Tip Chord	1 ft 11.5 in.
Overall Span	27 ft 4 in.
Total Exposed Area	58 ft ²
Incidence	8 deg
Dihedral	10 deg
Quarter Chord Sweep	10 deg 1.5 min
Taper Ratio (Exposed)	0.44
Aspect Ratio	8.0

Wing (cont'd)

Airfoil Section, Root	NACA 4415
Airfoil Section, Tip	NACA 4415

Propulsion System

Engines	Two T58-GE-5
Takeoff Power (Eg. L.)	1500 HP
Military Power	1400 HP
Normal Power	1250 HP
Transmission Rating	2800 HP (111% engine torque)

Loading Conditions

Empty Weight*	10900 lb
Maximum Gross Weight Flown	18000 lb
Maximum Gross Weight Capability	21800 lb
Center-of-Gravity Range	258 in. to 276 in.

*Aircraft less fuel, payload, and crew.

THE S-67 SPEED BRAKE

Initial wind tunnel testing of a one-twelfth scale model of the S-67 evaluated an aerodynamic braking surface attached to the main landing gear (Reference 1). Evaluation of other speed brake locations (fuselage, wing, and ventral fin) indicated that wing-mounted surfaces were the most effective. Wind tunnel data predicted an increase of 1.5% in total aircraft drag at zero fuselage incidence. Moreover, wing lift could be reduced for better autorotation characteristics, and for roll control through asymmetric deployment.

Figure 2 shows the location and dimensions of the S-67 speed brakes. Figures 3 and 4 show in-flight front views of the aircraft clean and with brakes extended. The unperforated brake panels lie flush with the wing surface under normal flight conditions, and extend to a position at right angles to the wing chordline. All brake surfaces are actuated by a single hydraulic actuator. Normal time for opening or closing brakes is 1.2 seconds. The actuator control is in the pilot's collective stick, and the emergency retraction switch is on the emergency panel (Figure 5).

Wind tunnel data are presented in Appendix I, showing the effects of the wing and speed brakes on total aircraft lift, pitching moment, and drag, as a function of fuselage attitude, α_f , relative to the free stream.

FLIGHT TEST CONDITIONS

LOADING

Listed below are the combinations of gross weight and center-of-gravity locations that were flown. A forward center of gravity, at 10 percent of the weight, was not flown because it could only tolerate a very low tail load. However, this loading condition was investigated by the evaluation study.

<u>Load Condition</u>	<u>Gross Weight</u>	<u>Tail Load</u>
#1	17,500	"
#2	16,800	"
#3	17,300	"

FLIGHT

In-flight gross weight varied to 17,300 lb. with the highest tail load at an altitude of 3600 feet. For the high descent rate investigation, the descent study, it was necessary to commence partial power deceleration at a test altitude of 6000 feet.

STABILATOR FLAP ANGLE

The stabilator flap angle of 10 degrees leading edge down was determined for level flight with speed brakes retracted. This setting provided an overall minimum level of flap; toe and main rotor vibration, adequate longitudinal control margin, and a 10° pitch angle for positive stability with lift at high speeds. Reference is made to the report of the evaluation study for the effects of stabilator flap angle.

卷之三

卷之三

Figures 4, 5, and 7 compare aircraft positions and aircraft attitudes with and without speedbrakes extended. When the speedbrakes are extended, a nose-down pitching moment results. To arrest for this, changes in longitudinal cyclic pitch of less than 1% are required. The expense for the loss in wing lift is negligible ($\Delta C_L \approx 0$).

新嘉坡華南銀行有限公司

At speeds between 10 and 15 ft/sec, all three engine torque settings for each flow speed, the torque ratio available required for level flight, the maximum torque available, 1.65 kg, and an intermediate torque setting. Thus, engine torque, flow speed, and aircraft speed were obtained at a constant flow angle of attack. Figures 1a, 1b, and 1c show wind charts for the 10, 12.5, and 15 ft/sec conditions with aircraft traces extended, and the 10, 12.5, and 15 ft/sec condition with just aircraft traces extended. Figures 2a and 2b show schematically the values of δ_{a} , δ_{m} , and δ_{e} for minimum trim angle at a silent speed of 10, 12.5, and 15 ft/sec aircraft traces retracted and extended. Figure 3 shows the resulting desired aircraft trim angle of attack and trim angle.

In addition to the aircraft attitude, flight path, it is important if the pilot is to control the aircraft, to know the aircraft's position relative to the ground. The five charts derived from flight test data, in Figure 10, show altitude, horizontal distance, time, airspeed, and vertical velocity. Variations in all five. These data are used as input to the computer to determine the aircraft's position relative to the steepness of the terrain as the aircraft flies over a hilly or mountainous area. These data, if constant, are used to predict flight test data; however, if no predictable variations in the terrain are present, no information will be

It is feasible to limit the variation of α by as much as possible and in particular to prevent the variation of aspect ratio, but with sufficient rotation, it is still feasible to increase visibility and the angle of approach. However, it is also observed that, for a given wing aspect ratio, smaller leading edge flaps are less significantly effective than larger flaps. Figure 11 shows the variation of aspect ratio of a typical aircraft with and without flaps extended, showing that it is possible to achieve a reduction of the aspect ratio of 10% with little effect on the aspect ratio of the aircraft. The leading edge flap is located ahead of the trailing edge flap (near the root). The relative angle of attack of flaps is such that it reduces the angle of attack of the aspect ratio which is significant in reducing the drag coefficient.

The five aircraft considered were the A-4, A-7, A-10, F/A-18, and F/A-16. In addition, four aircraft configurations were simulated, the configuration being the aircraft with its landing gear retracted. Therefore, a total of ten aircraft configurations were considered.

Because the aircraft configurations and aircraft speeds used were not retracted were not initially concentrated at flight test sites, the performance results of the aircraft programs. These results are shown in Figures 14 and 15. The results of flight test data with the simulation are summarized in Appendix III. Correspondingly, the configuration of the transonic-centered cruise in simulation was compared to the flight test data with simulated data for cruise power, center of gravity, and aircraft attitudes. For this reason, cruise power in Figure 15 is unity as much as 1%.

Maine turbine pressure is a function of altitude plus constant terms, as shown in Figure 16, and plots for the A-4, A-7, and A-10 aircraft in Figure 17, speed transients extended. The total speeds in Figures 14, 15, and 16 are constant speeds. For each aircraft, flight test data is normally

RESULTS

Flight test results also calculated at the cruise, as defined by stress and center flatness limits, which are discussed below. Data were not taken at the same speeds shown in Figures 14, 15, and 16. Figures 14, 15, and 16 show how the individual transients selectively describe several points of Figures 17 and 18, at a rate of 10°/sec. at a constant free angle retracted. With brakes extended, Figure 18, the maximum free angle is 10 degrees, also at 10°/sec. In contrast to Figures 14 and 16, at the lighter aircraft, at the same speed and engine power, and to about 10 degrees less.

In all cases shown, dives are at a faster rate than with even steeper dives feasible if the aircraft is permitted to accelerate. The flatness limits are too restrictive for supersonic free flight, and must be circumvented.

Free angles selected must be consistent with the calculated free dives. This is particularly important in the case of the A-10 aircraft, in which the free angle is limited to 10°. The other aircraft have larger free angles (present brakes at 10°) and are not limited to constraints as the A-10.

Maximum engine torque limit

An engine output power limit of 100% is implemented in the Transonic CFD code. This corresponds to 100% engine RPM.

Maximum angle of attack limit

As the angle of attack increased from 0° to about 15° forward of vertical, the main rotor tended to autorotate. A maximum angle of attack limit was established at the main rotor stall angle of approximately 15° forward of vertical, and the rotor would stop. At this point, the main rotor torque, or thrust, would become zero. If the aircraft had sufficient lift, this stall regime was acceptable, and it was determined by the lack of initial climb performance. A constant angle of attack was used for each plane. The main reason for this was that the dependence of the aircraft's aircraft weight and center of gravity on lateral position and roll angle, which is a function of the roll angle and pitch, did not change significantly at the designated flight condition of 10° angle of attack.

The first stability criterion of interest was that the aircraft would not roll up or down, and secondly, the aircraft would not autorotate. At about 15° of angle of attack, the main rotor stalled, and the aircraft began to roll. It was determined that as the angle of attack increased, the effect of the main rotor torque decreased, so that as the angle of attack increased, the effect of the main rotor force decreased, and the aircraft would roll. In addition, the aircraft would roll up at 15° of angle of attack, so that the aircraft would roll up.

Maximum lateral limit

At least one roll axis limit must be imposed, and this is the lateral limit. This limit is also imposed to prevent the aircraft from rolling excessively. The lateral limit affects the lateral position of the aircraft around its center of gravity. Finally, the lateral limit of the aircraft is imposed to prevent the aircraft from rolling excessively.

Maximum roll rate limit

With a roll rate criterion, the aircraft must not roll too fast. This is another safety criterion that prevents the aircraft from rolling excessively. The lateral position of the aircraft is controlled by the lateral position of the aircraft, and the roll rate is controlled by the roll rate of the aircraft. The roll rate of the aircraft is controlled by the roll rate of the aircraft, and the lateral position of the aircraft is controlled by the lateral position of the aircraft.

Implementation of the roll rate limit is done by calculating the roll rate of the aircraft, and then setting a limit on the roll rate. The roll rate is calculated by the roll rate of the aircraft, and the lateral position of the aircraft is calculated by the lateral position of the aircraft.

Lack of flight pedal control

The CH-47 has a cambered vertical tail surface to reduce tail rotor torque requirements in high-speed level flight. As the aircraft accelerates in a dive and main rotor torque is reduced, more right pitch is required to offset the side force caused by the vertical tail surface. Referring to Figure 10, as engine torque is decreased at constant airspeed, the tail rotor blade pitch angle approaches the negative limit of -7 degrees to maintain trim. Reference 3 specifies a control margin of 10% of travel, so that tail rotor blade angle should not exceed -4 degrees.

This limitation may be eased by extending the tail rotor negative pitch limit. If no undesirable tail rotor instabilities develop, pitch negative blade pitch. Alternatively, the center of the vertical fin might be reduced. This would lead to greater tail rotor thrust in level flight, with associated penalties in forward speed capability and tail rotor stresses. In any case, if a rudder were eliminated, a replacement for the yaw control system.

Tail rotor extension and retraction, steady flight

The aircraft transient responses to speed brake extension with fixed controls were obtained at speeds from 100 to 170 mph. Figure 11 shows time histories for a speed of 170 mph. The speed is constant at 170 mph and 100% wing lift as brakes are extended twice in a sequence, and after about 1 second the aircraft approaches 10 degrees nose-down in pitch and about 5 degrees left in roll. The transient response of speed brake retraction during a steady dive results in a nose-up pitching moment that improves the "pull-up" capability of the aircraft.

Deceleration, Aileron trim

Decelerations from 170 mph with speed brakes retracted and extended were performed at constant altitude with aileron trim, aileron stick was held constant, and roll speed was 10 degrees. Figure 12 shows time histories of the deceleration with speed brakes retracted. Because of the constant altitude constraint, aileron deflection was constant and aileron roll angle was held as the aircraft pitch was controlled by reducing collective. Total time for the maneuver was 1.6 seconds. Figure 13 presents data with speed brakes extended. At first, aileron trim was set to 0 degrees for the roll axis, so wing left aileron trim was 10 degrees. This was achieved with aileron stick held. The maneuver was then repeated with aileron trim set to 10 degrees. The time constant of aileron was 1.6 seconds. Maneuvers were also performed with aileron trim at -10 degrees trim, with speed brakes, and aileron trim was 10 degrees. The 10 degree trim was the minimum trim value. At time t = 0, aileron stick was held constant, and aileron trim was set to 10 degrees. At 1.6 seconds, aileron trim was set to -10 degrees. Maneuver was at 170 mph initial. Mean values for the 10-degree trim run were 1.6 sec.

One decelerating left turn was performed from 160 knots to 100 knots, using speed brakes. Deceleration time was 10.6 seconds, including a 1.2-second delay after brake extension before rolling into the turn. Brake retraction was initiated after passing 60-degree bank, which increased pitch rate and load factor. Thereafter, aft cyclic and down collective were employed to complete the maneuver. Mean turn radius was 530 feet. Main rotor pushrod loads were at approximately the same level as on previous turns, but stationary control loads were 50-60% higher.

COMPUTER SIMULATION STUDY

Appendix II describes the computer simulation and shows the comparison of simulation data with flight test data. The simulation was used to predict the effects on dive characteristics of increased brake effectiveness and stabilator bias angle, and to briefly study asymmetric brake deployment. The light aft load condition (2) was used, with a stabilator bias angle of 2.5 degrees.

Increased Brake Effectiveness

Figures 14 and 15, previously mentioned, show dive angle and fuselage angle of attack information developed at the 14,800-lb aft (#2) load condition with and without speed brakes. Figures 15 and 22 illustrate the effects of increased brake effectiveness. Additional brake area should be located on the lower ventral fin, where drag forces would align the airframe to the flight path, and turbulence would not impinge on any control surfaces. The simulation results show that a dive angle of 30 degrees is possible at 160 knots. Also, the increased brake area further reduces variation in fuselage angle of attack.

Effect of Stabilator Bias Angle

The fuselage attitude, α_f , was nose up relative to the flight path in a trimmed dive and varied with speed and rate of descent, reaching about 15 degrees at minimum torque. The speed brakes reduced angle of attack by up to 4 degrees (Figure 12), at a given dive angle and speed, but greater pitch control can be attained by varying stabilator bias angle.

The dive characteristics were established using the simulator with a stabilator bias angle of 2.5 degrees leading edge up, relative to the neutral position, rather than the 1.5-degree flight test bias angle, to determine any significant change in angle of attack. From Figures 15 and 16, angle of attack is reduced by as much as 4 degrees when stabilator bias is increased from 1.5 to 2.5 degrees.

Asymmetric Deployment

A short study was conducted to predict the consequences of asymmetric speed brake deployment due to actuator malfunction. The simulator was used to determine controllability in high-speed level flight with every configuration of extended brake surfaces. Identification of the six brake surfaces is consistent with the original wind tunnel nomenclature Reference 1, and is shown in Figure 24.

Because of the asymmetry of lateral/directional control, the ability to trim the aircraft differs when considering left or right brake extensions. The simulations showed that when brakes are asymmetrically deployed, at forward speeds up to 180 knots, there is always sufficient roll control power to retrim the aircraft, although some deceleration will occur due to available power and/or collective limits. For example, if surfaces 1, 2, and 5 are opened at a forward speed of 180 knots, while 3, 4, and 6 remain closed, the aircraft will decelerate to about 160 knots because of the engine power limit, with the pilot able to restore and hold the aircraft at zero roll angle. At entry speeds below 145 knots, trim can be restored at the same speed following any configuration of speed brake deployment.

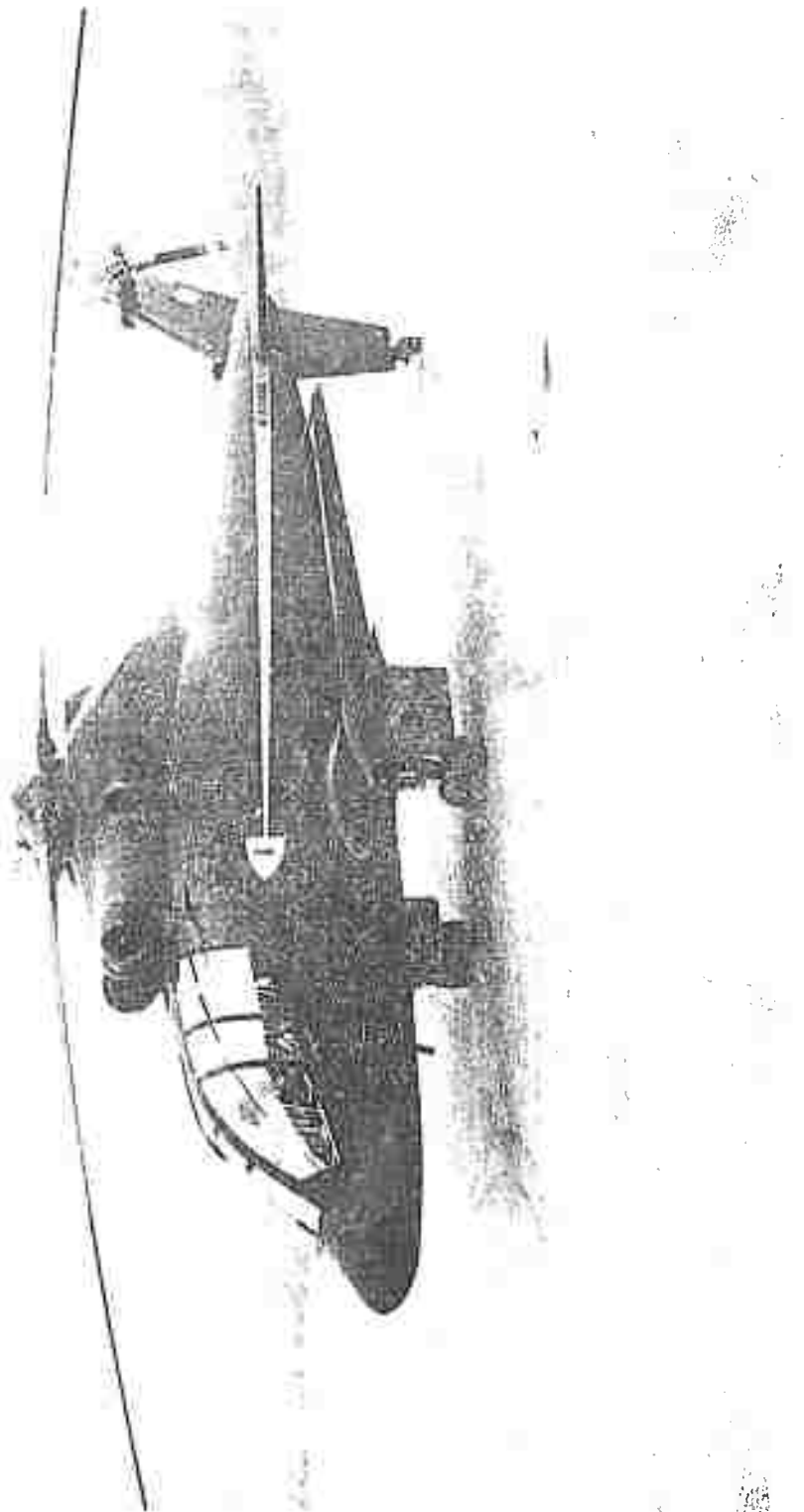
CONCLUSIONS

The wing-mounted speed brakes on the S-67 aircraft increase dive angle and reduce the fuselage attitude relative to the flight path (fuselage angle of attack). They permit increases in dive angles from 5 to 7 degrees at 140 knots dependent upon the initial dive angle. At 160 knots, the increase in dive angle varies from 8 to 9 degrees. The increases in aircraft dive angle due to speed brake extension can be further increased if the aircraft is allowed to accelerate in the dive. For dive speeds greater than 120 knots, the fuselage angle of attack is reduced 4 to 5 degrees by extending the speed brakes. The increase in dive angle and/or the reduction in fuselage angle of attack while maintaining airspeed by the use of speed brakes improve the S-67 aircraft's capability as a weapons platform.

LITERATURE CITED

1. Gifford, J. A., ONE-TWELFTH SCALE WIND TUNNEL TESTS ON THE AH-3 (S-67) DEMONSTRATOR AIRCRAFT, SER-67000, Sikorsky Aircraft Division of United Aircraft Corporation, Stratford, Connecticut, April 1970.
2. Kaplita, T. T., S-67 STABILATOR INVESTIGATION, SER-67006, Sikorsky Aircraft Division of United Aircraft Corporation, Stratford, Connecticut, June 1971.
3. GENERAL REQUIREMENTS FOR HELICOPTER FLYING AND GROUND HANDLING QUALITIES, MIL-H-8501A, Amendment 1, April 1962.
4. Corso, J. J., and Kaplita, T. T., GENERAL HELICOPTER SIMULATION PROGRAM, SER 50542, Sikorsky Aircraft Division of United Aircraft Corporation, Stratford, Connecticut, May 1968 .

 Reproduced from
best available copy.



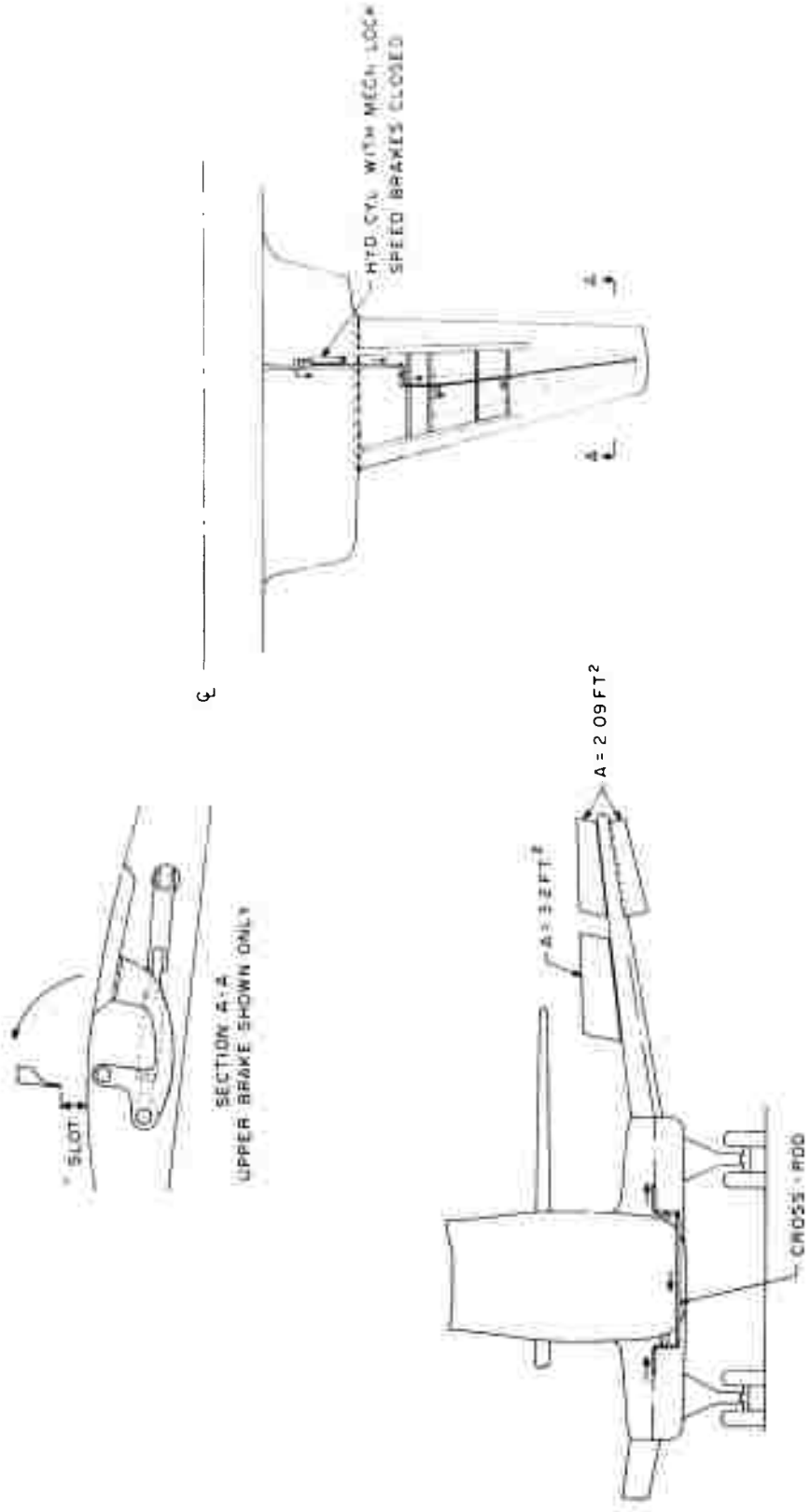


Figure 2. Speed Brake Areas and Locations.

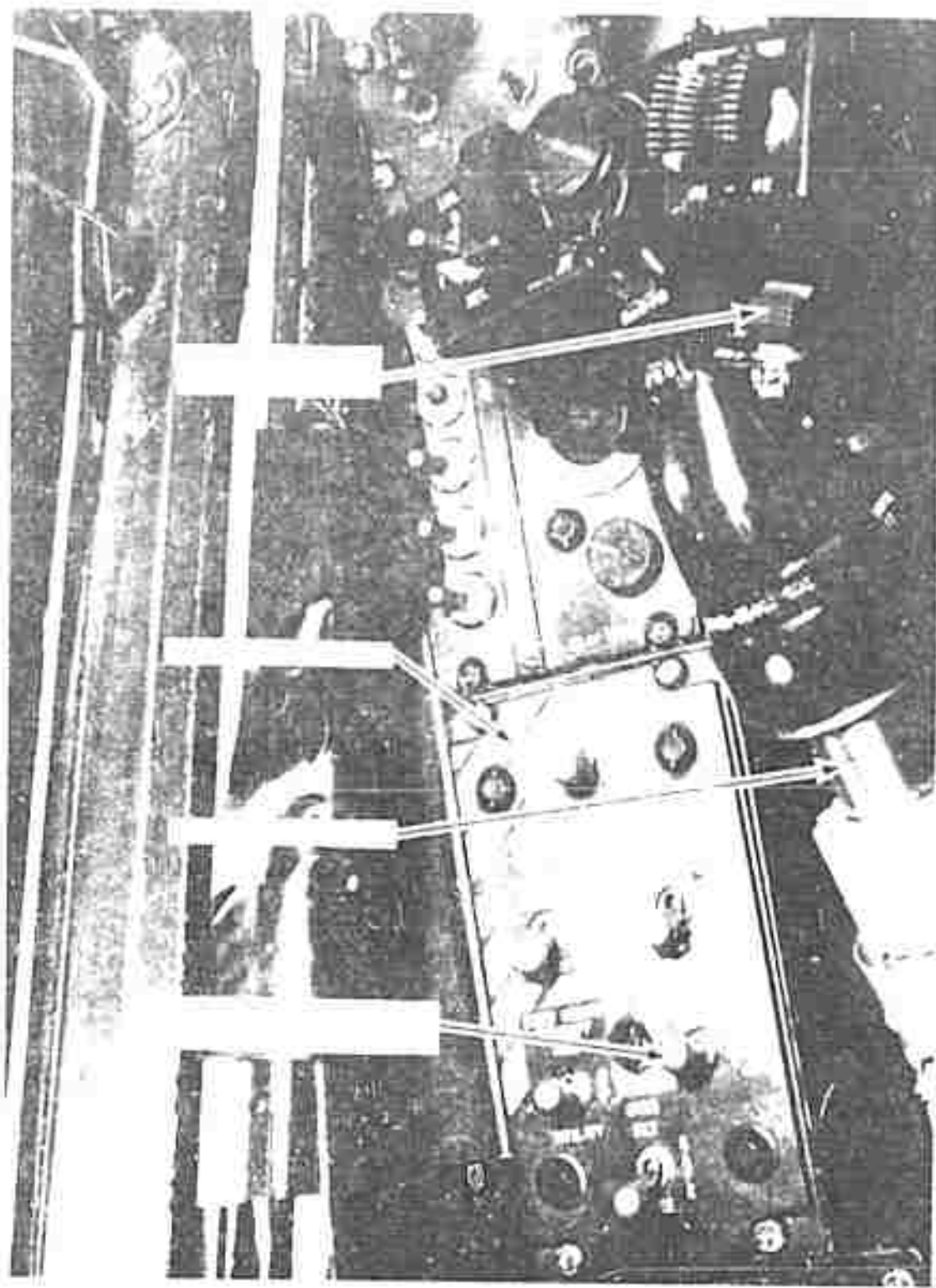


FIGURE 4. IN-FLIGHT FRONT VIEW OF A DOUGLASS C-47 SKYTRAIN AIRCRAFT.

Reproduced from
best available copy.



Figure 4. In-Flight Front View, Speed Brakes Extended.



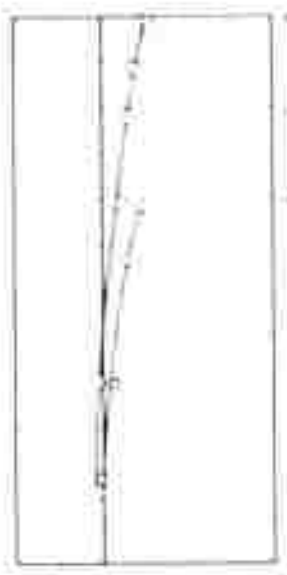
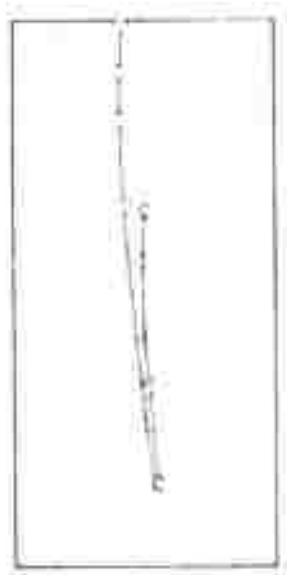
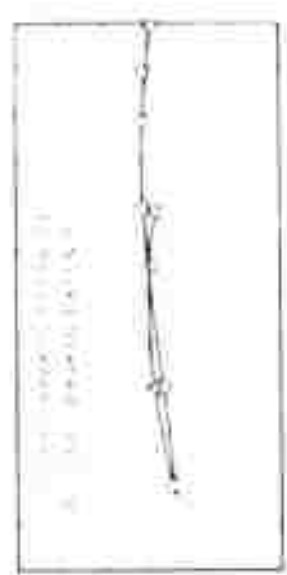


Fig. 1. Three types of curves

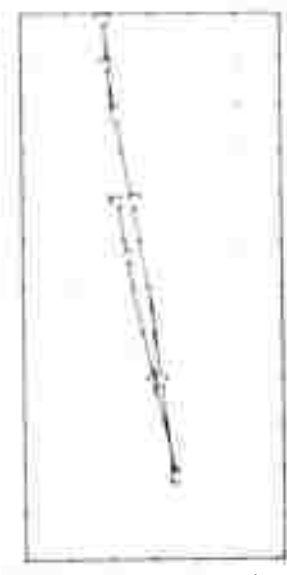
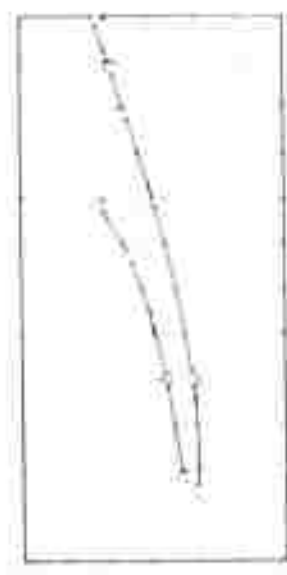


Fig. 2. Three types of curves



Fig. 1. Effect of temperature on the rate of reaction.



Fig. 2. Effect of temperature on the rate of reaction.

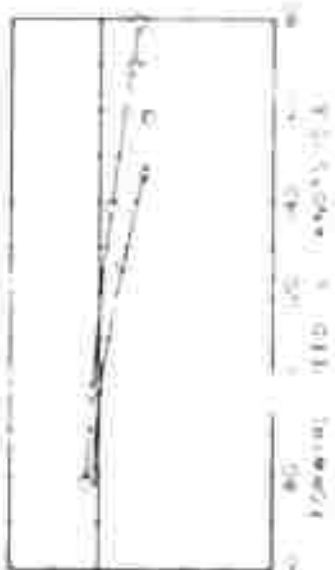


Fig. 3. Effect of temperature on the rate of reaction.

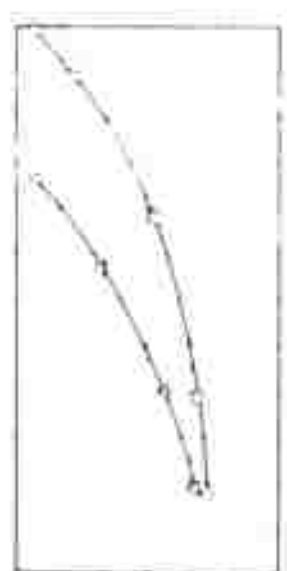


Fig. 4. Effect of temperature on the rate of reaction.

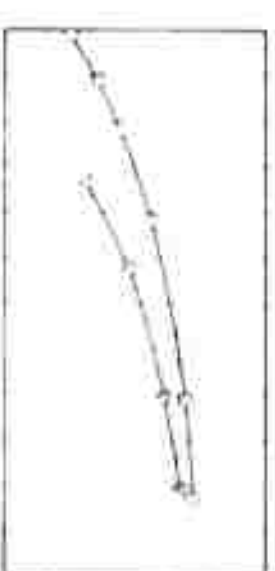


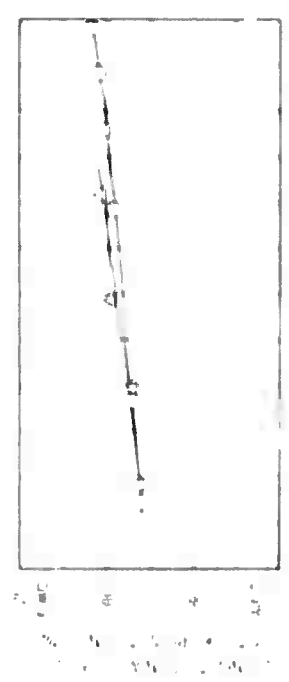
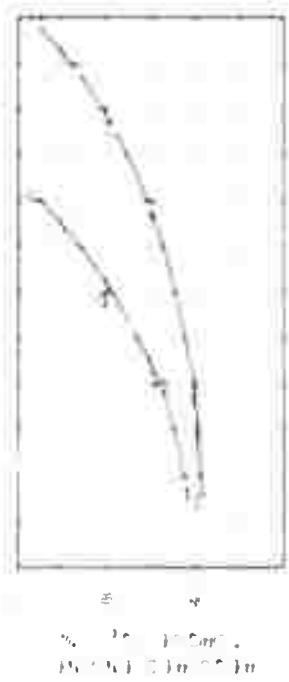
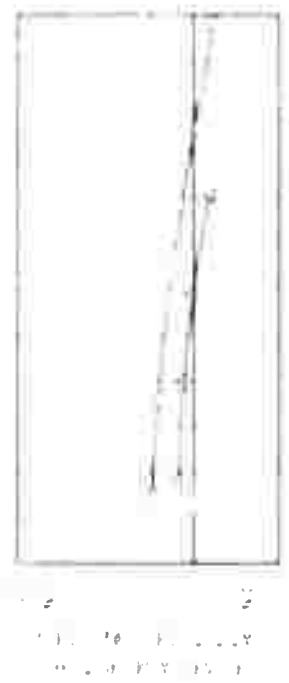
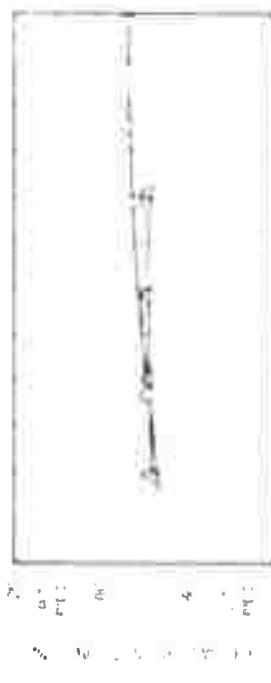
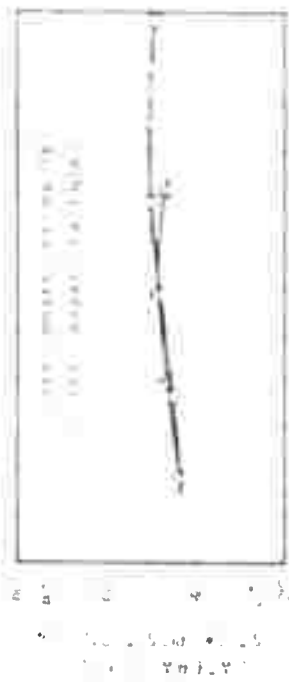
Fig. 5. Effect of temperature on the rate of reaction.



Fig. 6. Effect of temperature on the rate of reaction.

reaction. The results are shown in Figures 1-6. The control reaction is represented by a solid line and the heat-treated reaction by a dashed line.

The results show that the rate of reaction increases with temperature, and that the heat-treated reaction is significantly faster than the control reaction at temperatures above 60°C.



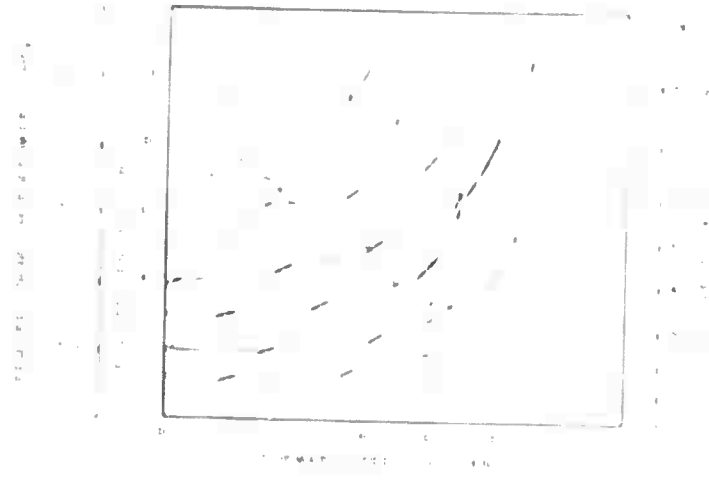


FIGURE 2. Correlation coefficients between the variables of the first (A) and second (B) groups.

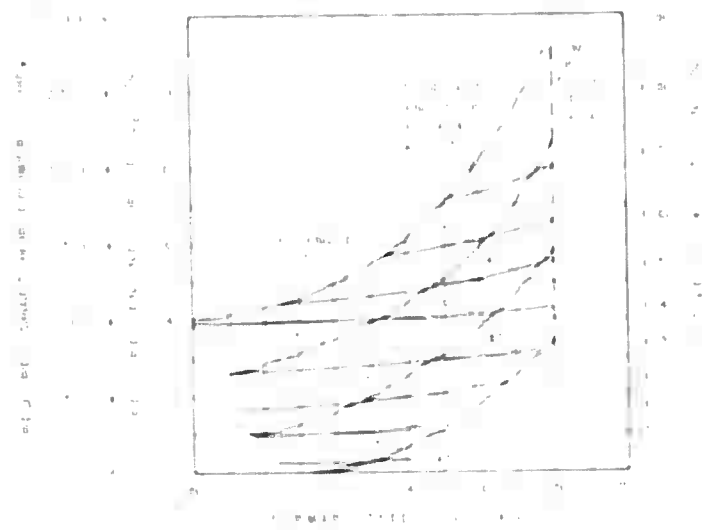


Fig. 1. Scatter plot of the relationship between the number of species

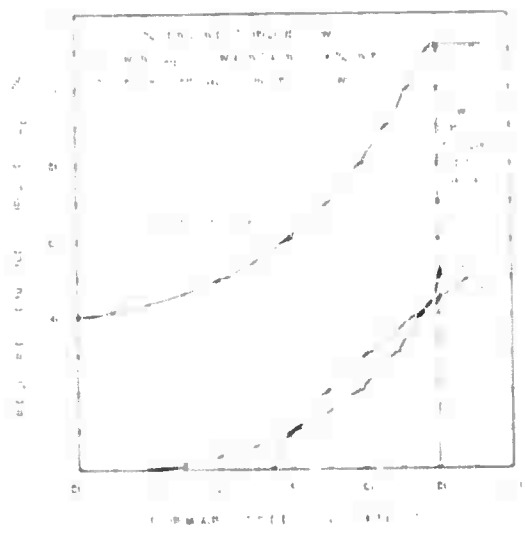


Fig. 2. Scatter plot of the relationship between the number of species

Figures 1 and 2. Scatter plots of the relationship between the number of species and the number of individuals in the data "original" and "modified" sets, respectively, for the first 100 data points.

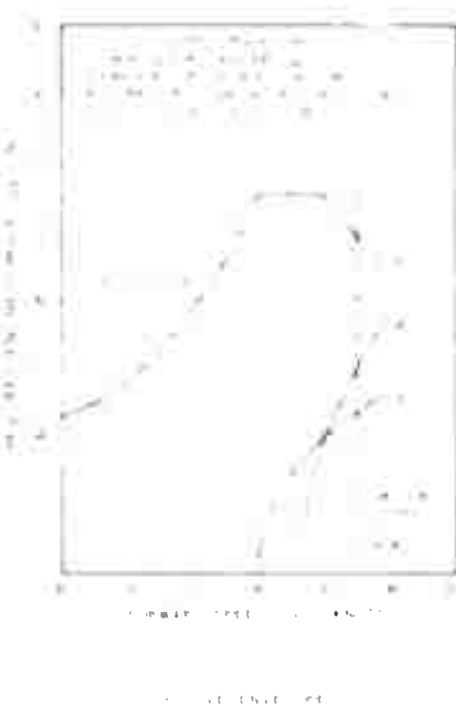
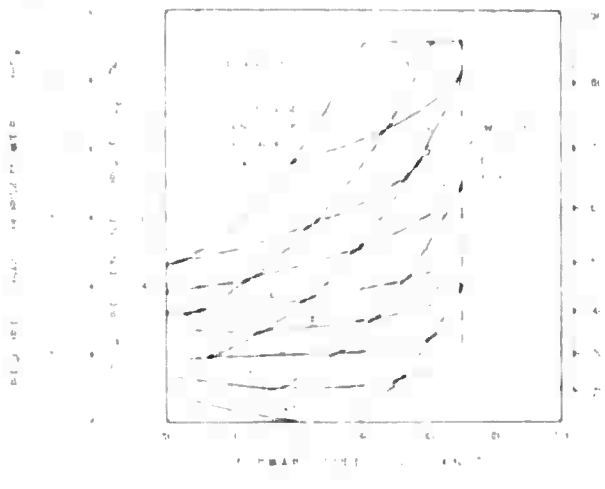
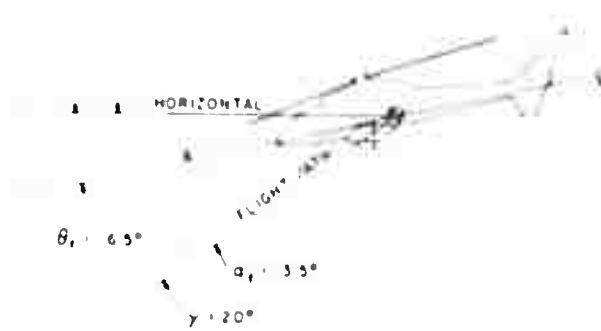


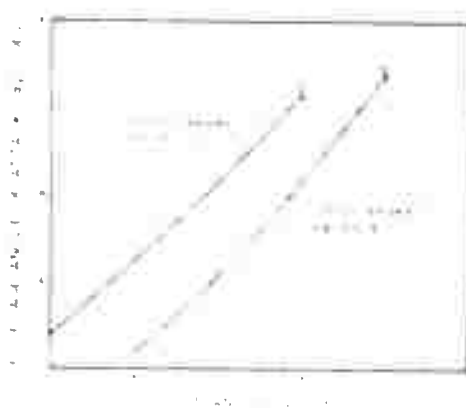
FIGURE 11. LIVE CHARACTERISTICS, $W = 11,300$ lb,
at 100% load, Jib Braces Extended.



(a) MAXIMUM DIVE ANGLE, SPEED BRAKES RETRACTED



(b) MAXIMUM DIVE ANGLE, SPEED BRAKES EXTENDED



(c) FUSELAGE ANGLE OF ATTACK VS DIVE ANGLE

Figure 10. Limiting Angles of Attack, $Ma = 1.7$, $L/D = 1.0$,
 $\beta^* = 17^\circ$, $\mu = 0.001$.

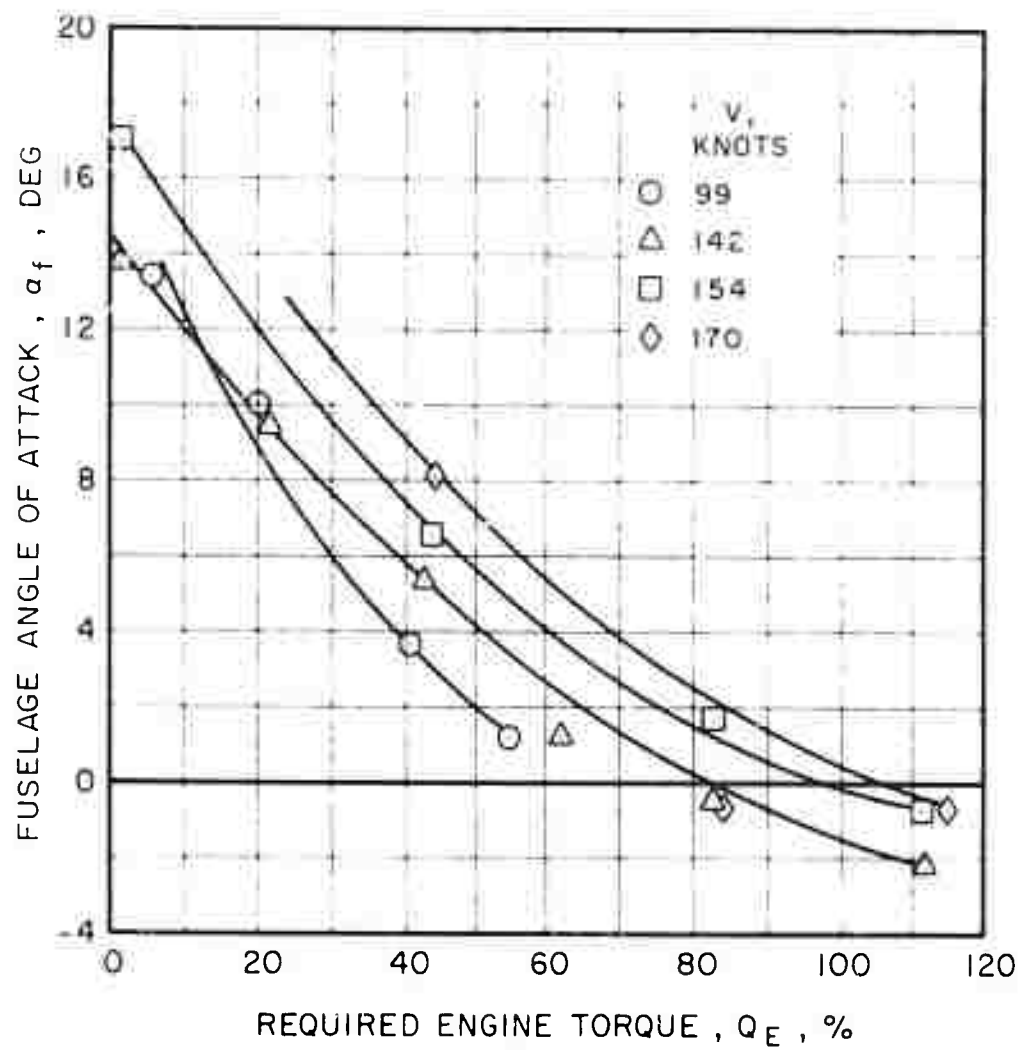


Figure 18. Fuselage Angle of Attack vs. Required Engine Torque and Forward Speed, $W = 17,400$ lb,
 $c_s = .75$ in., Speed Brakes Extended.

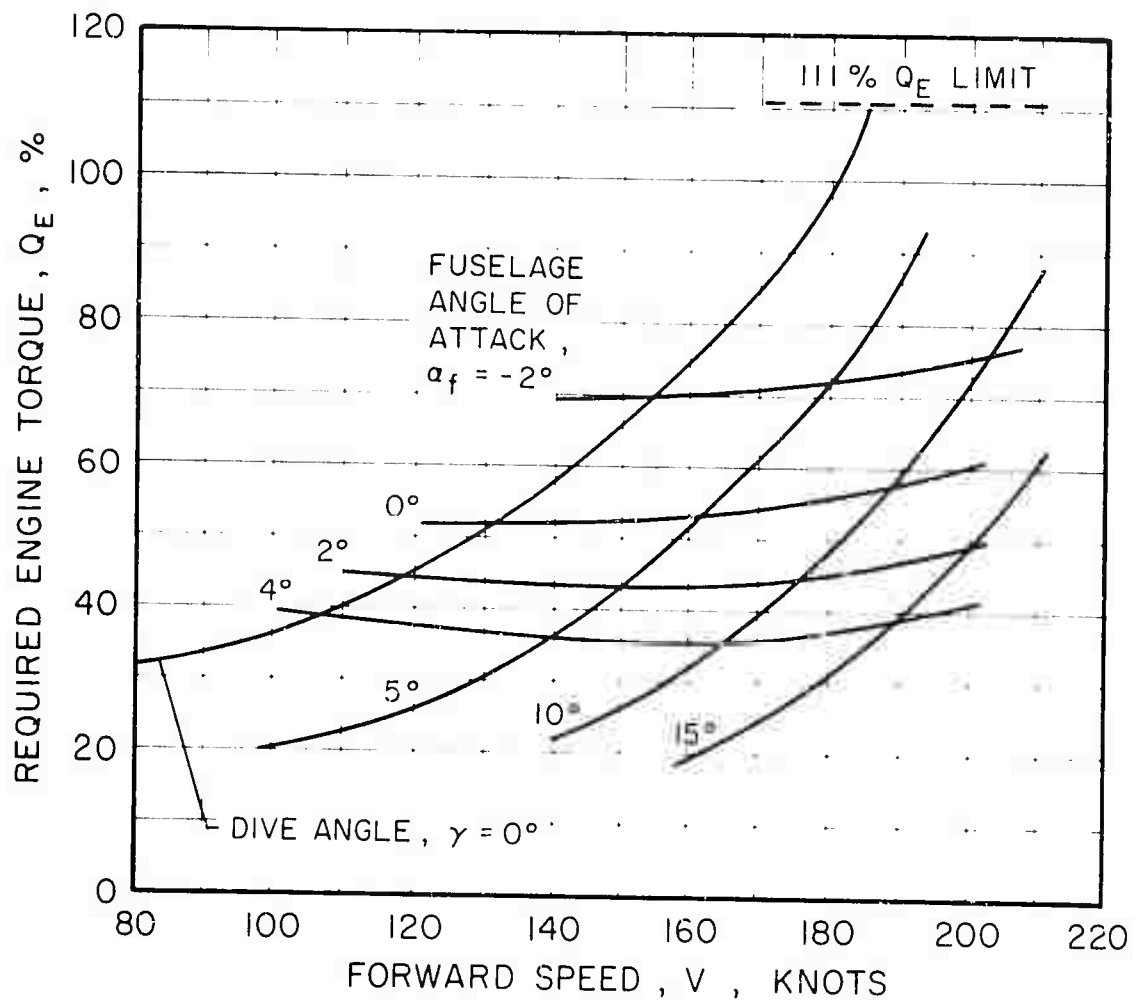


Figure 14. Simulation of Dive Characteristics, Speed Brakes Retracted, $GW = 14,800$ lb, $cg = 276$ in.

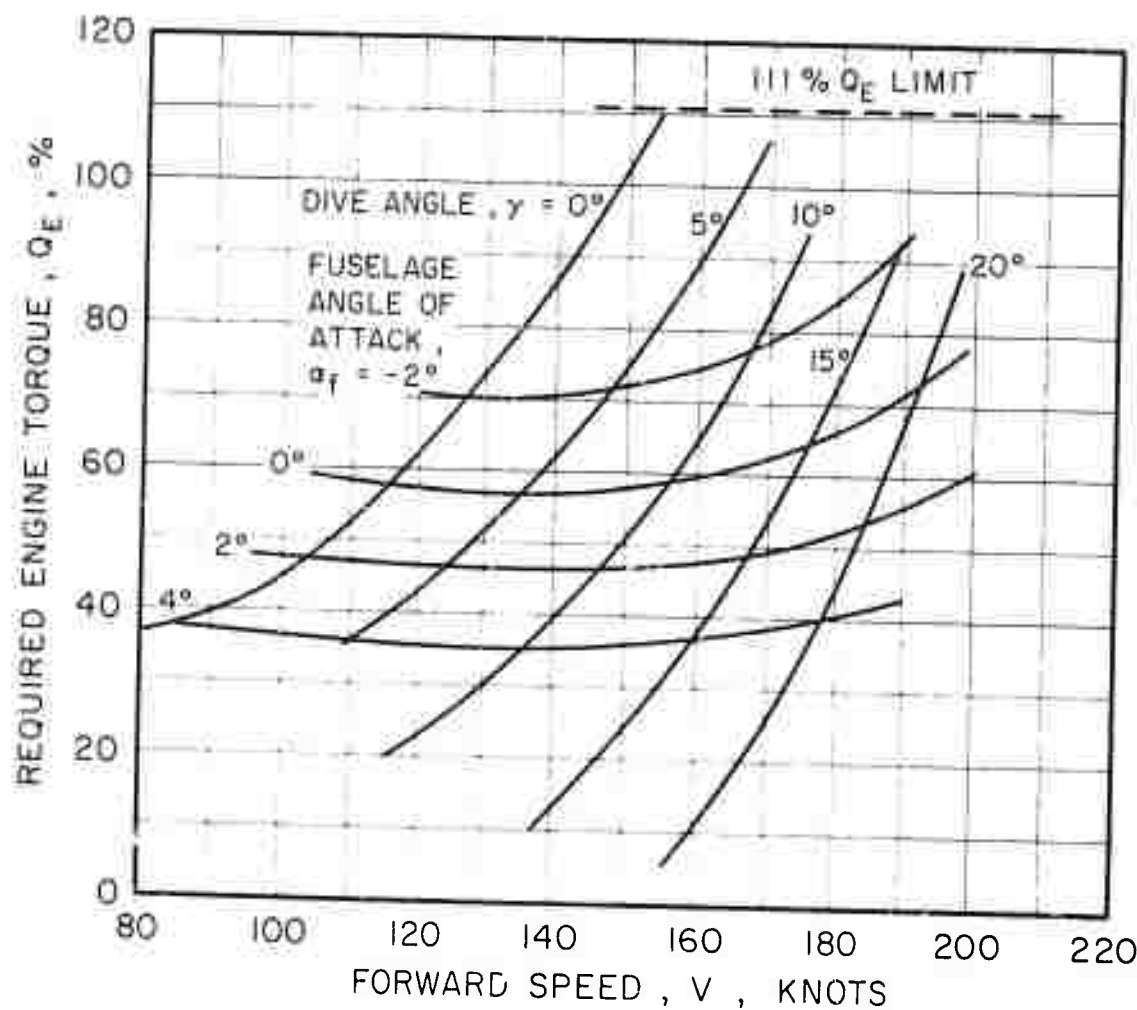


Figure 15. Simulation of Dive Characteristics, Speed Brakes Extended, $GW = 14,800$ lb, $cg = 276$ in.

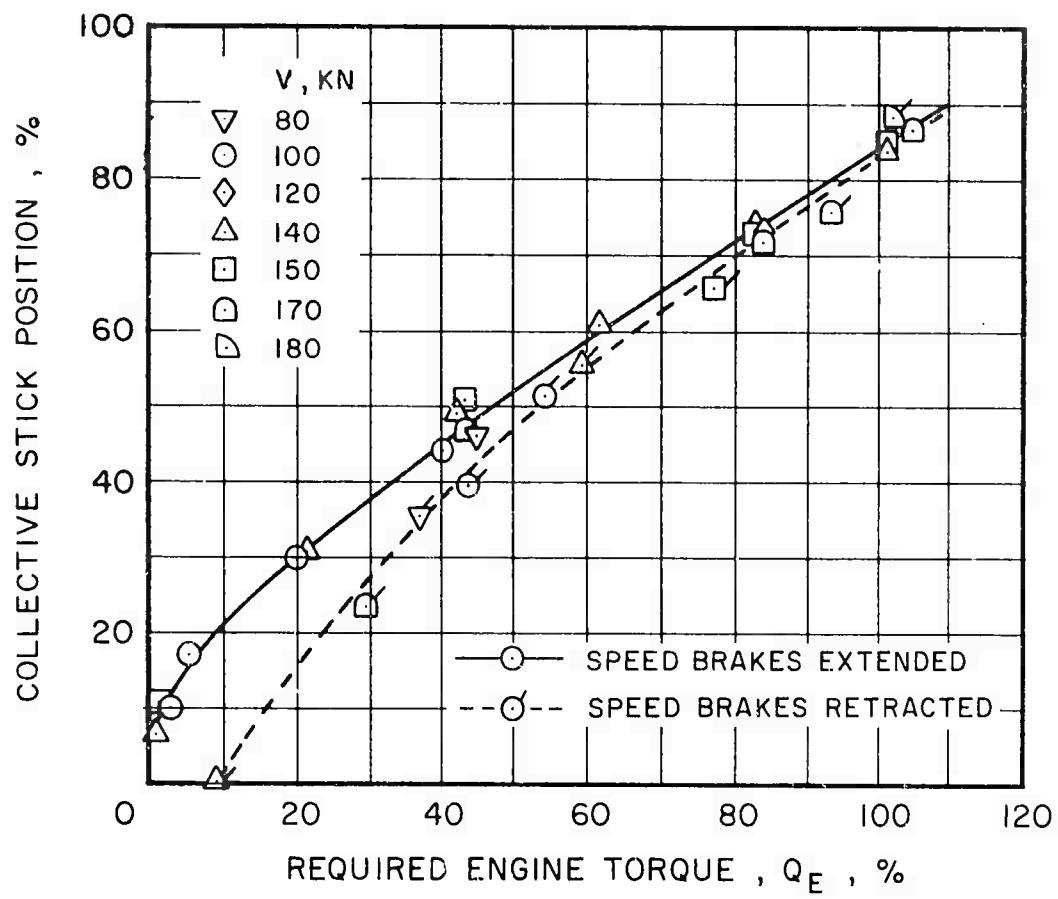


Figure 16. Collective vs. Engine Torque, GW = 17,300 lb,
cg = 276 in.

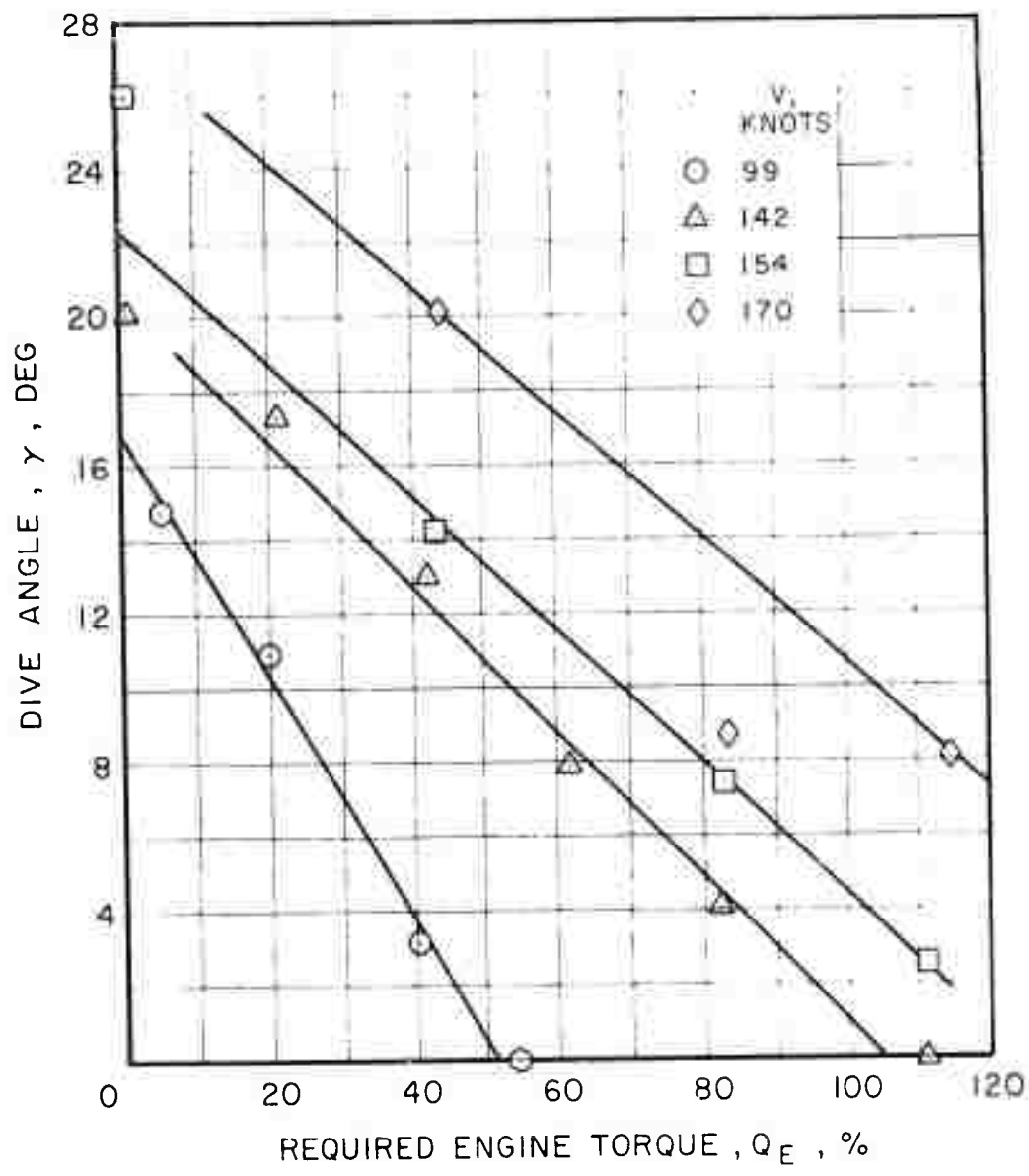


Figure 17. Dive Angle vs. Engine Torque and Airspeed, $G_W = 17,300$ lb, $c_g = .276$ in., Stabilizer Extended.

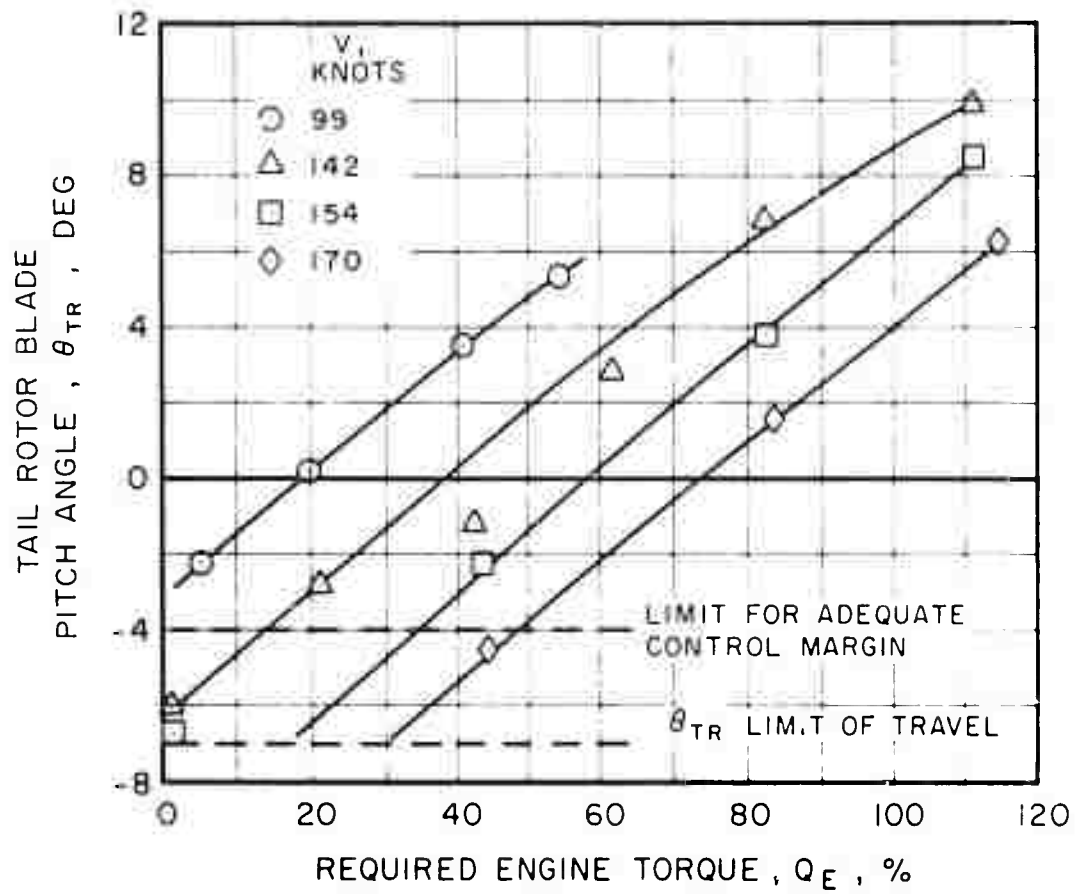


Figure 18. Tail Rotor Pitch vs. Engine Torque and Forward Speed, $W = 17,400 \text{ lb}$, $c_s = 30 \text{ in.}$, Speed brakes extended.

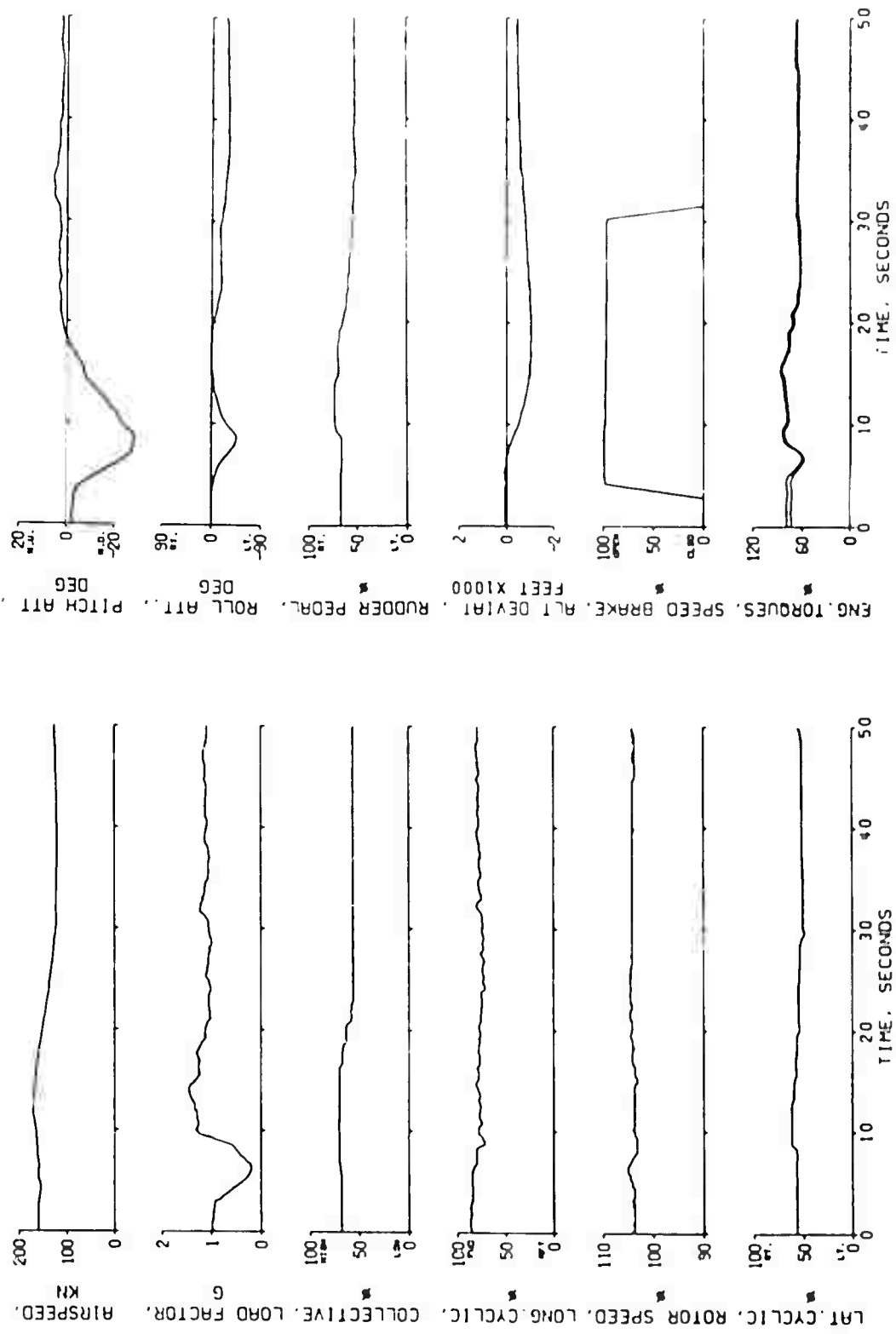
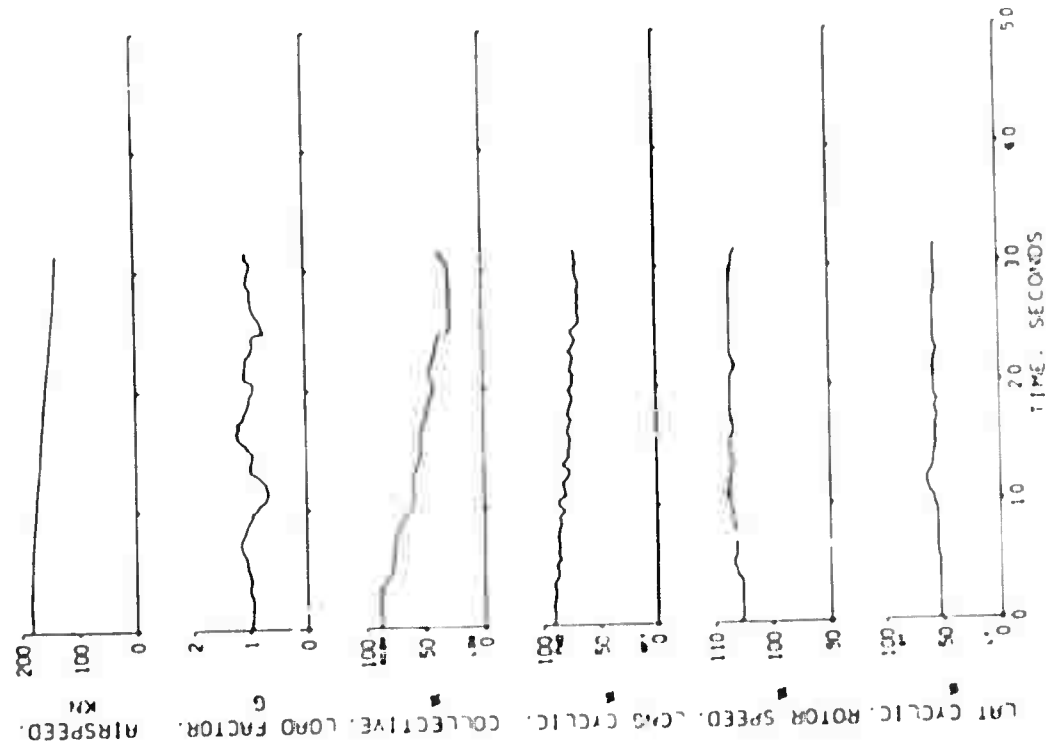
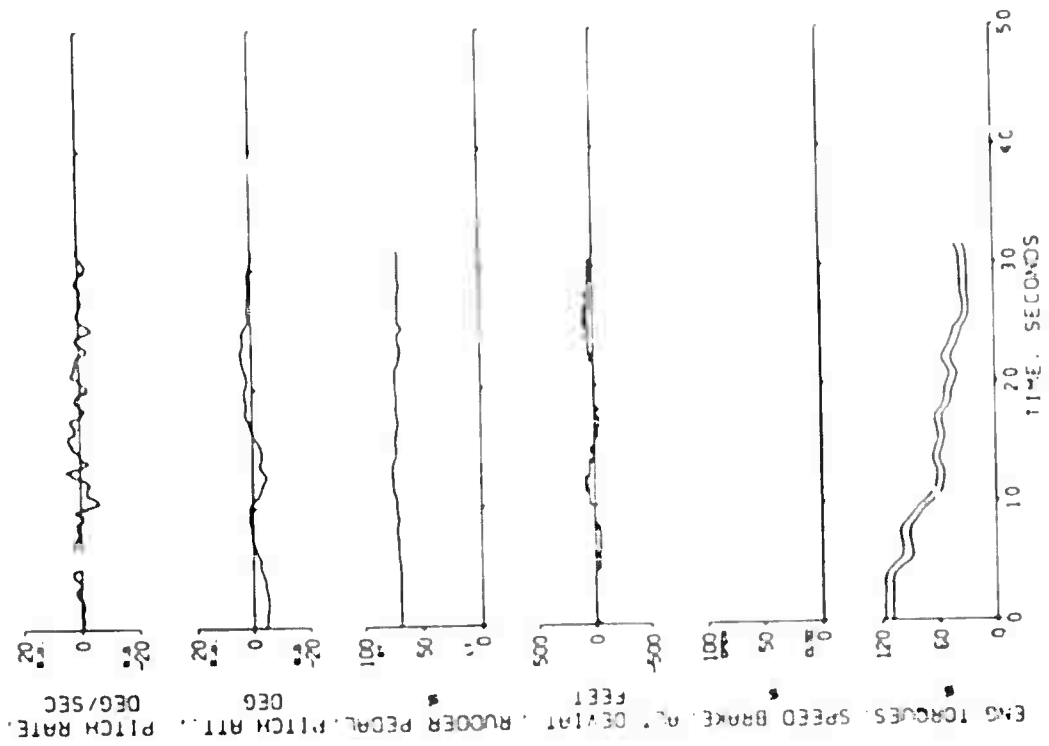
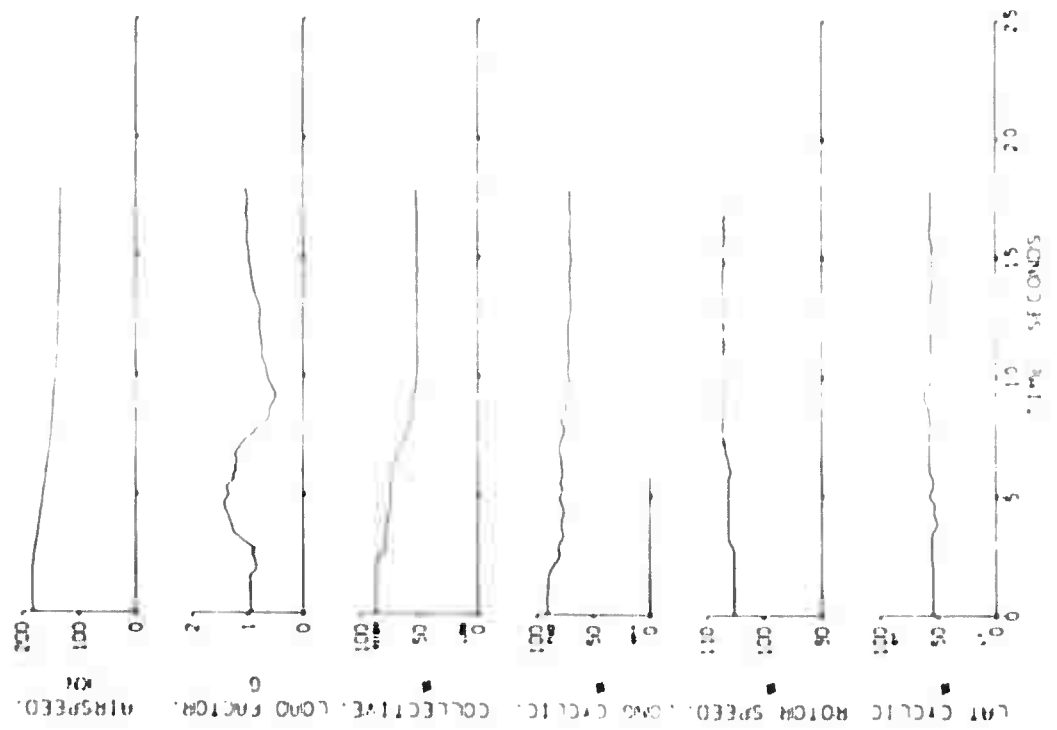
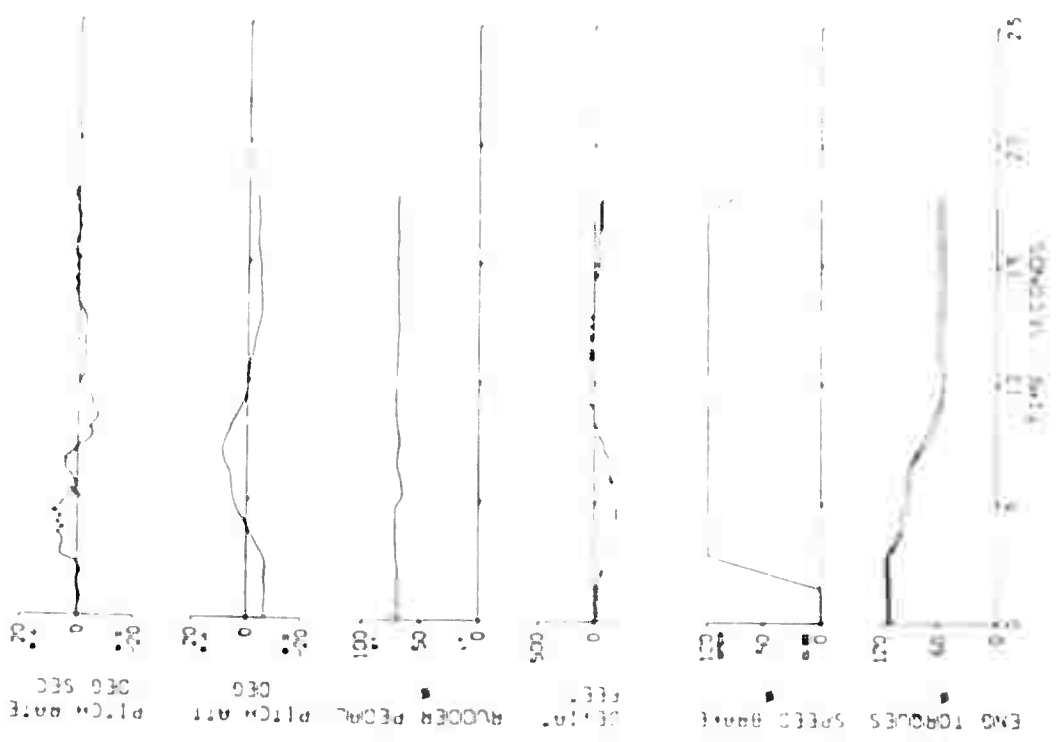


FIGURE 19. Transition Effects of Speed Brake Extension A.
 $V = 180 \text{ kt}$, Controls fixed.





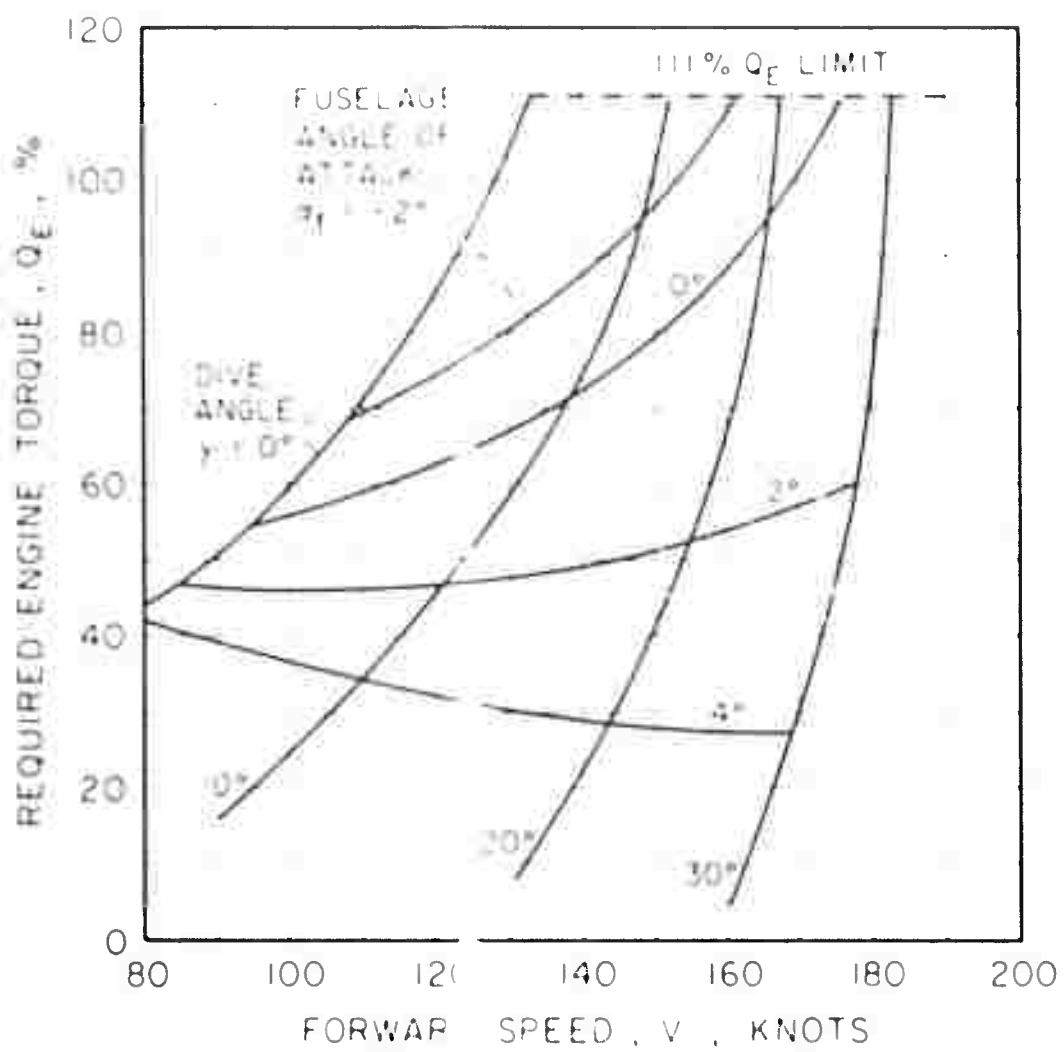


Figure 11. Variation of Dive Performance, Q_E , and Speed Limit, V , for a Jet, F-100, in the Reversing Power Area.

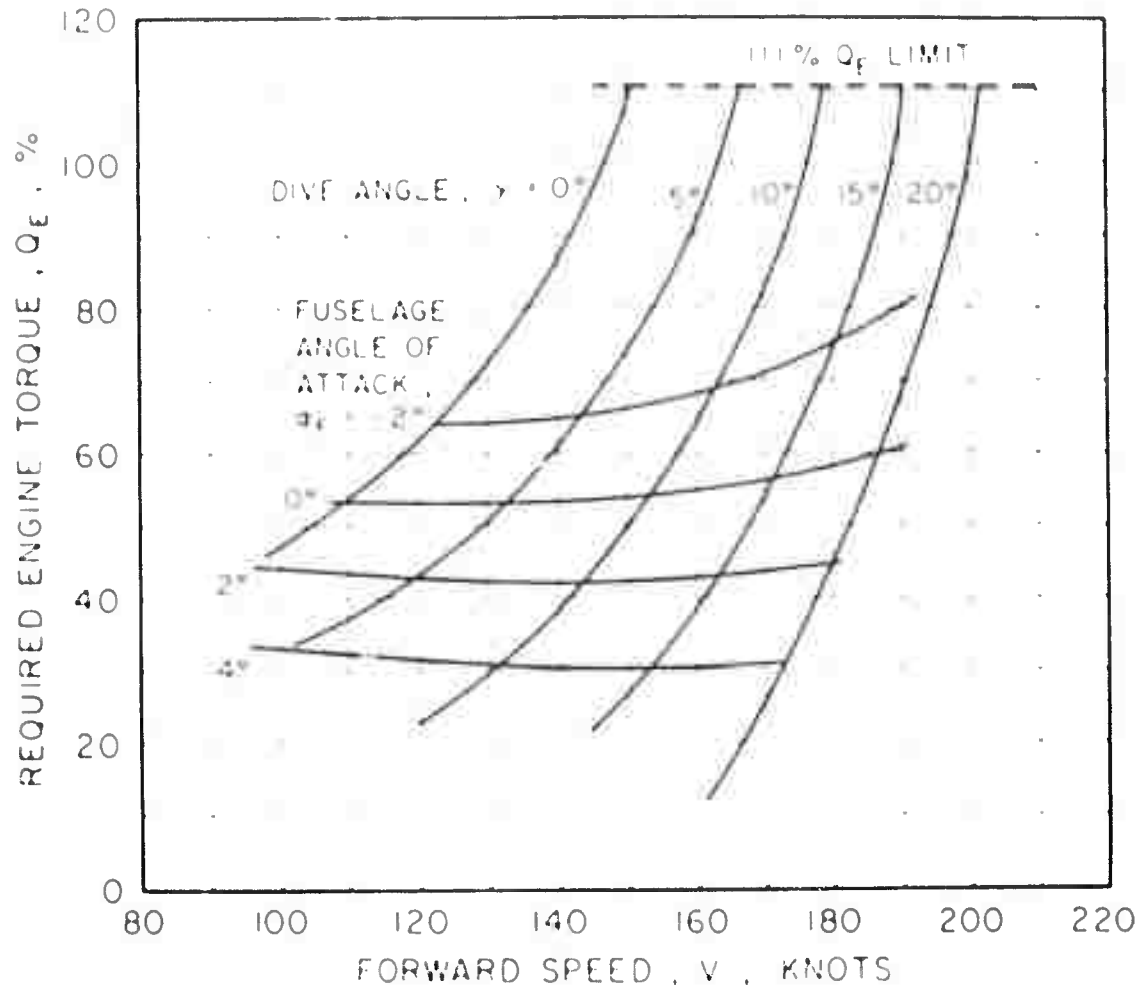
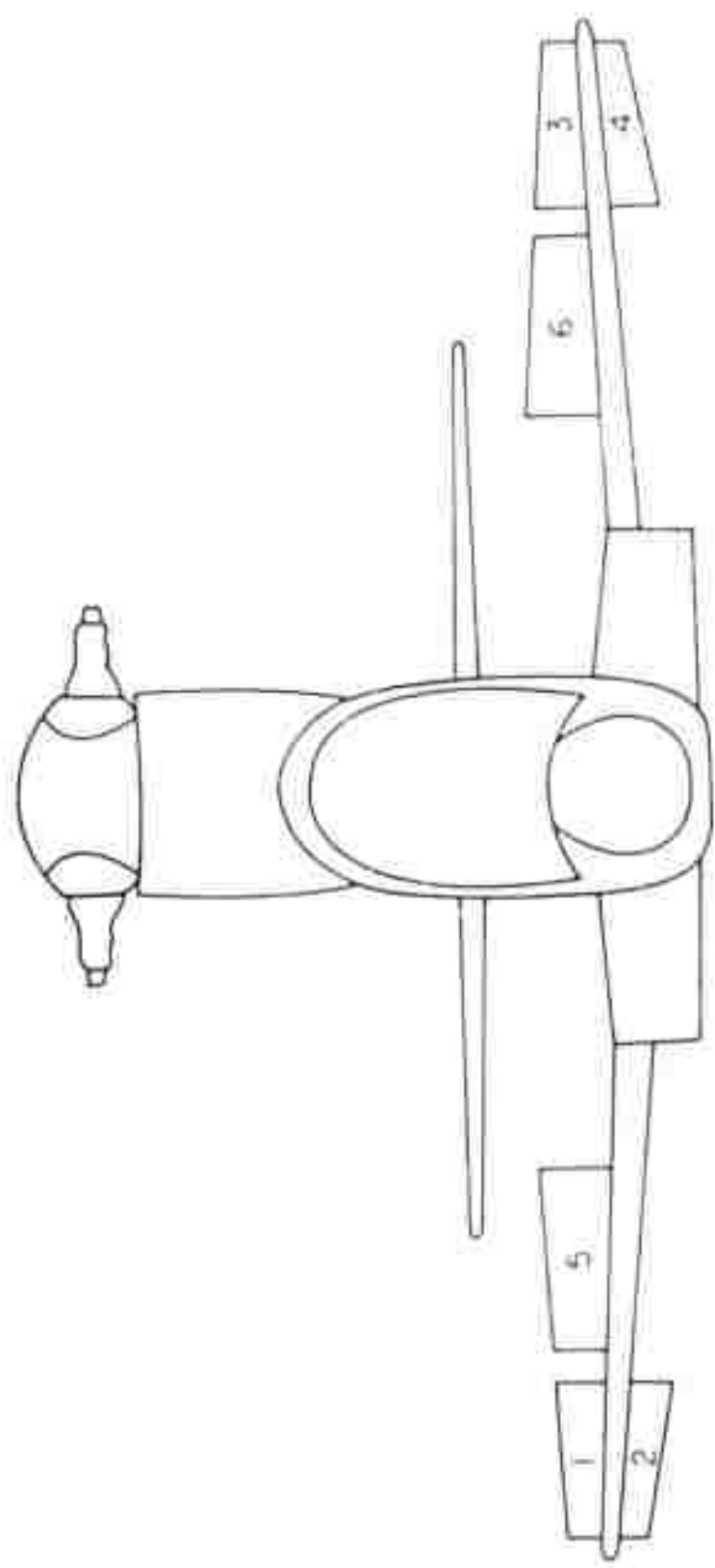


FIGURE 1. Required Engine Torque, Q_E , vs. Forward Speed, V , for Various Dive Angles and Fuselage Angles of Attack, with Brakes Locked, $W = 10,000$ lb., $S = 1000$ sq. ft., Initial Angle of Attack = 0° .



APPENDIX I

REFLECTIONS, PART

Figure 1 shows sample wind tunnel data traces for the effect of a change in pitching moment, M_{pq} , and drag area, A_D , parameters upon the variation of the angle of attack, α_p , at a tunnel speed of 10 ft/sec. The data were calculated for the basic airframe with 10% tail and 10% wing, and with wings and simulated trapezoidal surfaces added. The traces, originating at zero lift, produced a nose-down pitching moment variation of a 10° change in M_{pq} , and increased drag area by 10% at $\alpha_p = 10^\circ$.

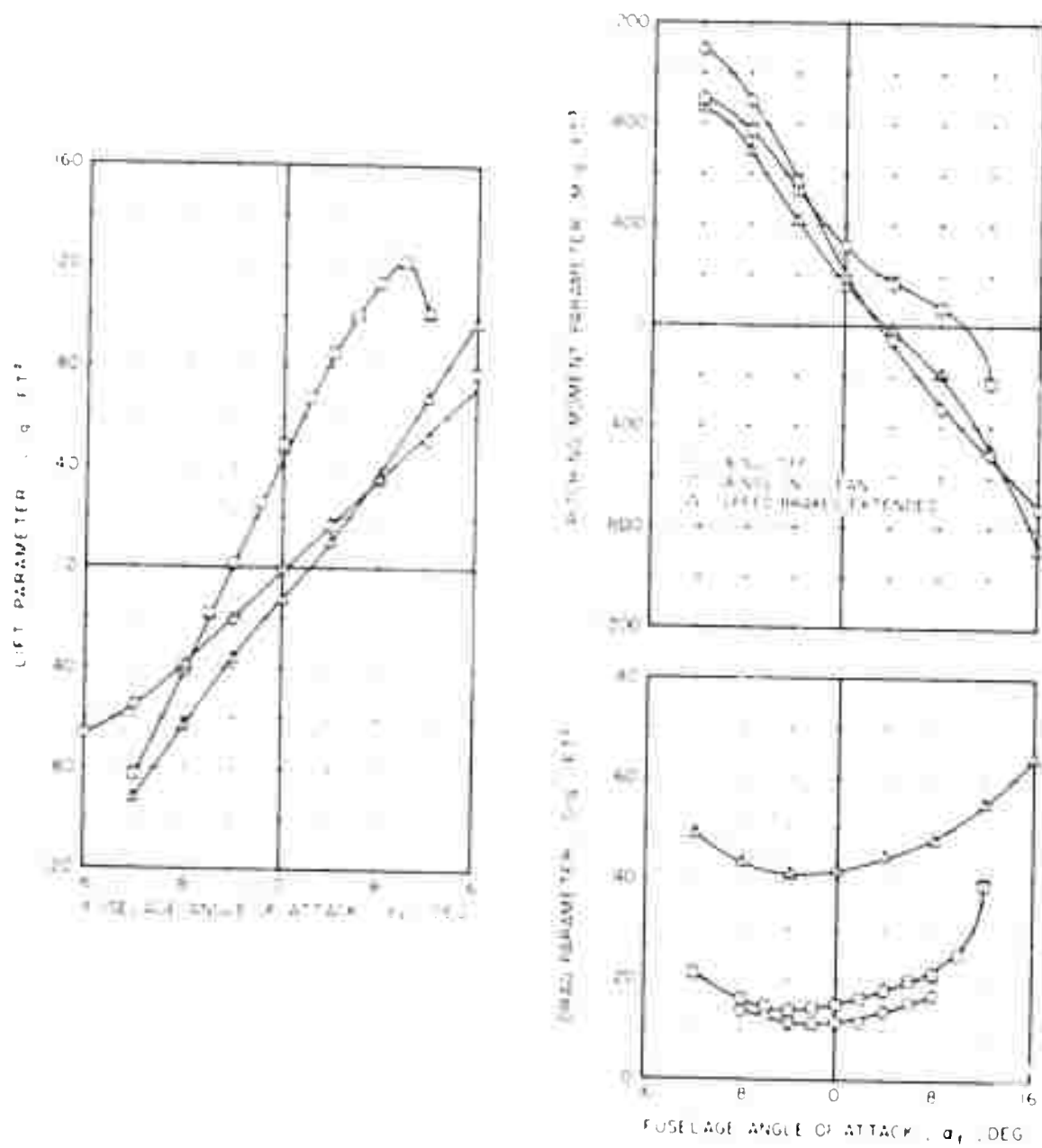


Figure 15. NACA Wind Tunnel Data, Showing Lift, Pitching Moment, and Trimming vs. Fuselage Angle of Attack for Total Aircraft Less Wings, With Wings and Speed Brakes Retracted and Extended.

APPENDIX II

COMPUTER SIMULATION STUDY

DESCRIPTION

The General Helicopter Simulation Program described in Reference 4 was adapted to Sikorsky Aircraft's PDP-10 digital computer to simulate the S-67. The six-degree-of-freedom simulation used a rotor model with a rigid five-bladed four-segmented blade element analysis including the rotor flapping degree of freedom. Nonlinear steady-state rotor blade airfoil section aerodynamic data were used that include the effects of stall and compressibility. Two-dimensional flow was assumed at each section of the blade.

Wind tunnel data from a one-twelfth scale model test of the S-67, Reference 1, were used to describe the force and moment contributions of the combined wing, fuselage, stabilator, and vertical tail. Speed brake contributions to the aircraft forces and moments were incorporated as additional components to those for the basic aircraft. The wind tunnel data included the effects of aircraft angle of attack and stabilator incidence on lift, drag, and pitching moment.

CORRELATION WITH FLIGHT TEST DATA

Hover

In hover, two adjustments to the simulation were necessary to obtain satisfactory correlation. Main rotor blade twist was increased by 2 degrees, and a 2-inch lateral center-of-gravity shift to the left was applied at the light gross weight conditions.

The S-67 rotor blades show some degree of aerodynamic twisting with the 20-degree swept tips. Under normal trimmed flight conditions, the blade loadings are high at the blade tip. Since the center of pressure of the swept tip is behind the blade torsional axis, aeroelastic twisting results.

The lateral center-of-gravity offset to the left brought the trim lateral cyclic requirement into agreement with flight test data. This center-of-gravity offset is expected, since the tail rotor and the vertical tail are positioned to the left of the aircraft centerline.

Forward Flight

In forward flight, the blade aerodynamic twist correction for collective pitch correlation varied with speeds above 80 knots. Above this speed the correction diminished linearly to -0.5 degree at 182 knots. A leading-edge-up stabilator bias angle correction of 2 degrees was needed to correlate longitudinal cyclic and aircraft attitude. This is due to some inaccuracies in predicting main rotor downwash at the stabilator.

Figure 26 shows the results of the correlation in hover and forward flight for the light-gross-weight aft-center-of-gravity condition, with speed brakes retracted and zero stabilator bias angle. Specific flight test points were simulated using the proper gross weight and density altitude. From hover to 80 knots, the simulation points are connected by a dotted line to indicate that no correlation was attempted in the low-speed regime.

At high speed, the rotor model requires extremely high power at moderate rotor stall. This is because two-dimensional flow at the rotor blade section was used, omitting the spanwise component.

To correlate flight test values of longitudinal cyclic and aircraft pitch attitude in forward flight with speed brakes extended, a reduction in the pitching moment was necessary, equivalent to that produced by 9 square feet of drag area. The wind tunnel model speed brakes were fixed flush to a solid wing, whereas the extended brakes on the S-67 leave a hole through the wing and a 1-inch slot between the brake panel and the wing, as shown in Figure 2. The resulting aerodynamic inconsistencies between wind tunnel and flight test conditions, and the shortcomings of the rotor model mentioned above, hindered exact simultaneous correlation of aircraft attitudes, control quantities and rotor power in level flight.

Figures 27 through 29 show the results of the correlation for different gross weights, center-of-gravity positions, and stabilator biases.

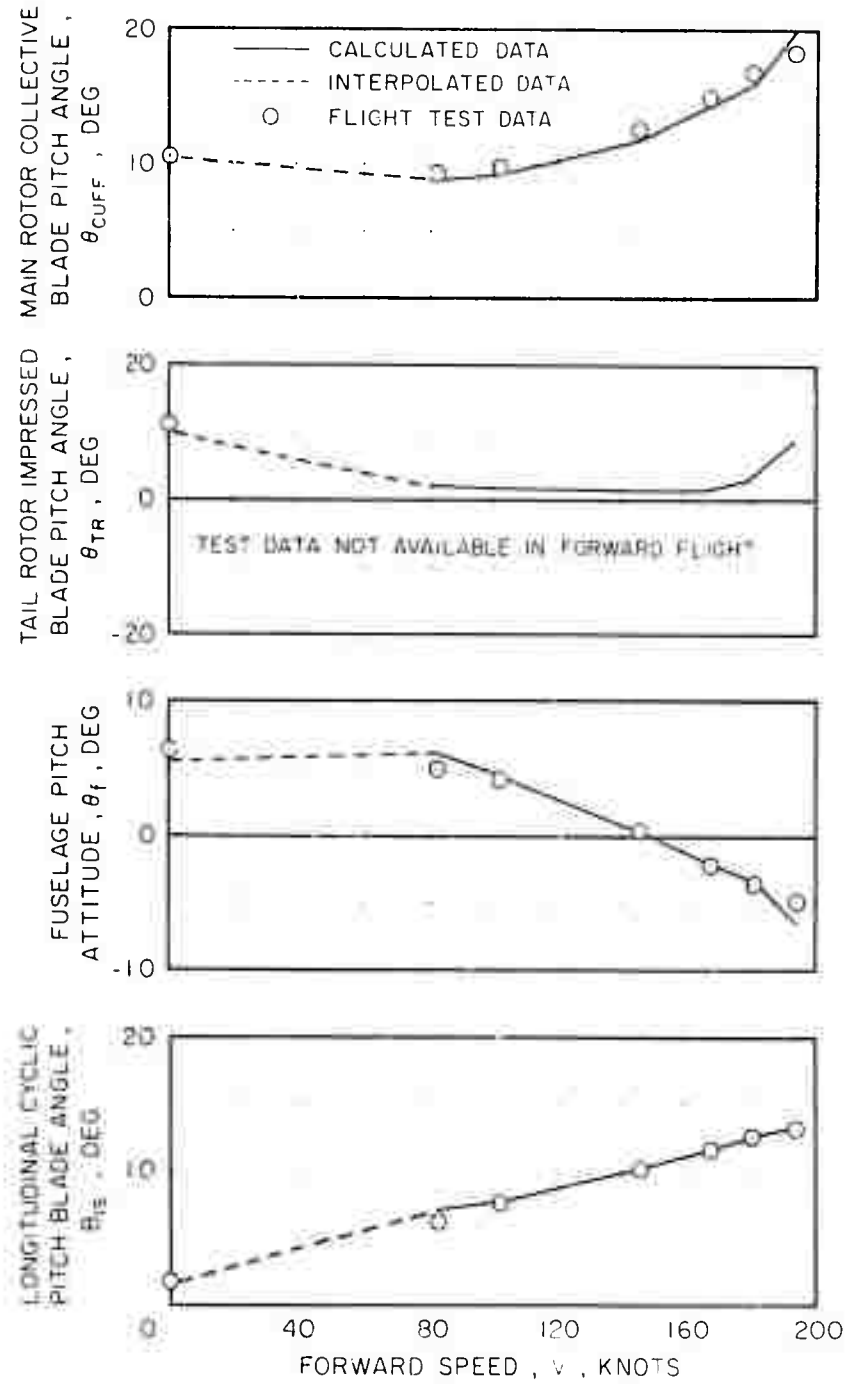


Figure 26. Comparison Between Simulated and Flight Test Data, Level Flight Trim, $GW = 10,000$ lb, $c_g = .70$ in., Stabilator Bias = 0 deg, Speed brakes retracted.

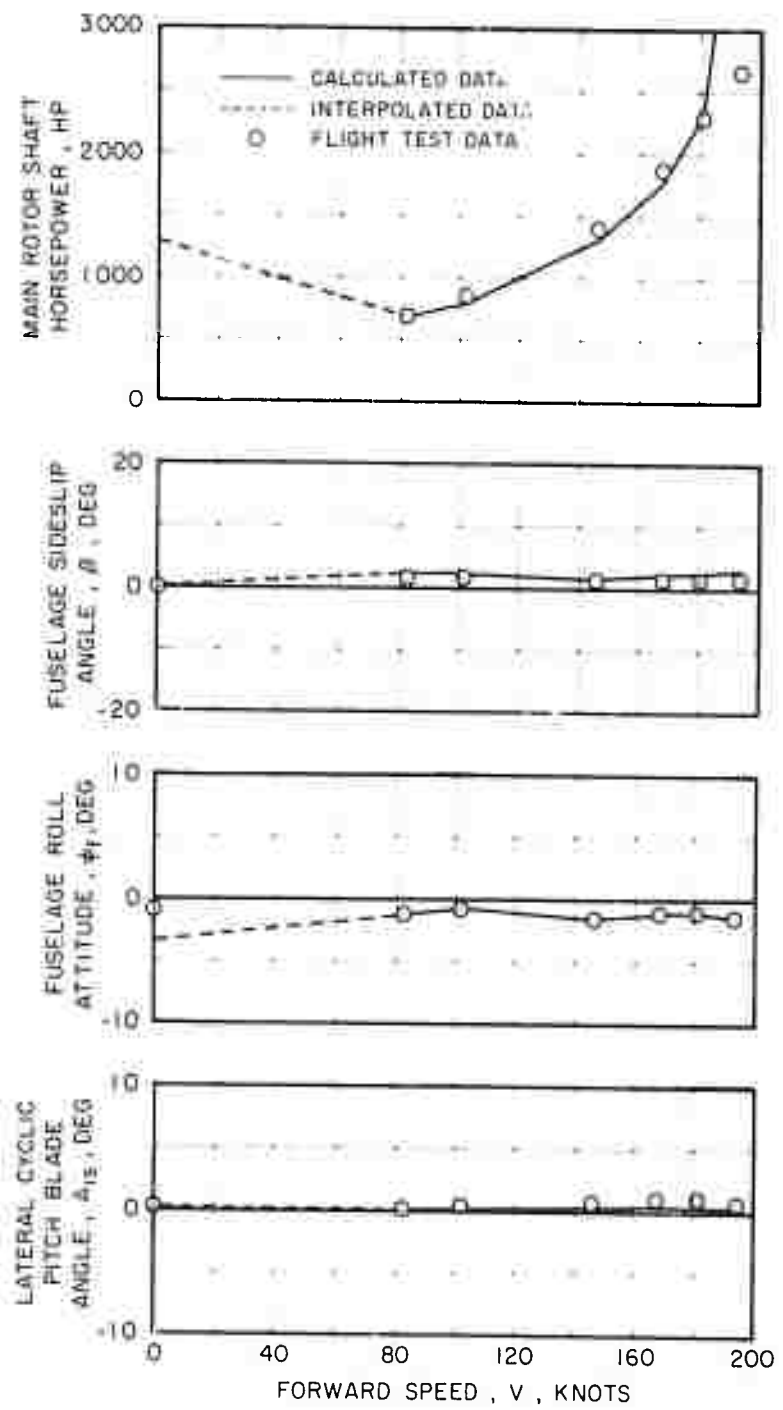


Figure 26. Concluded.

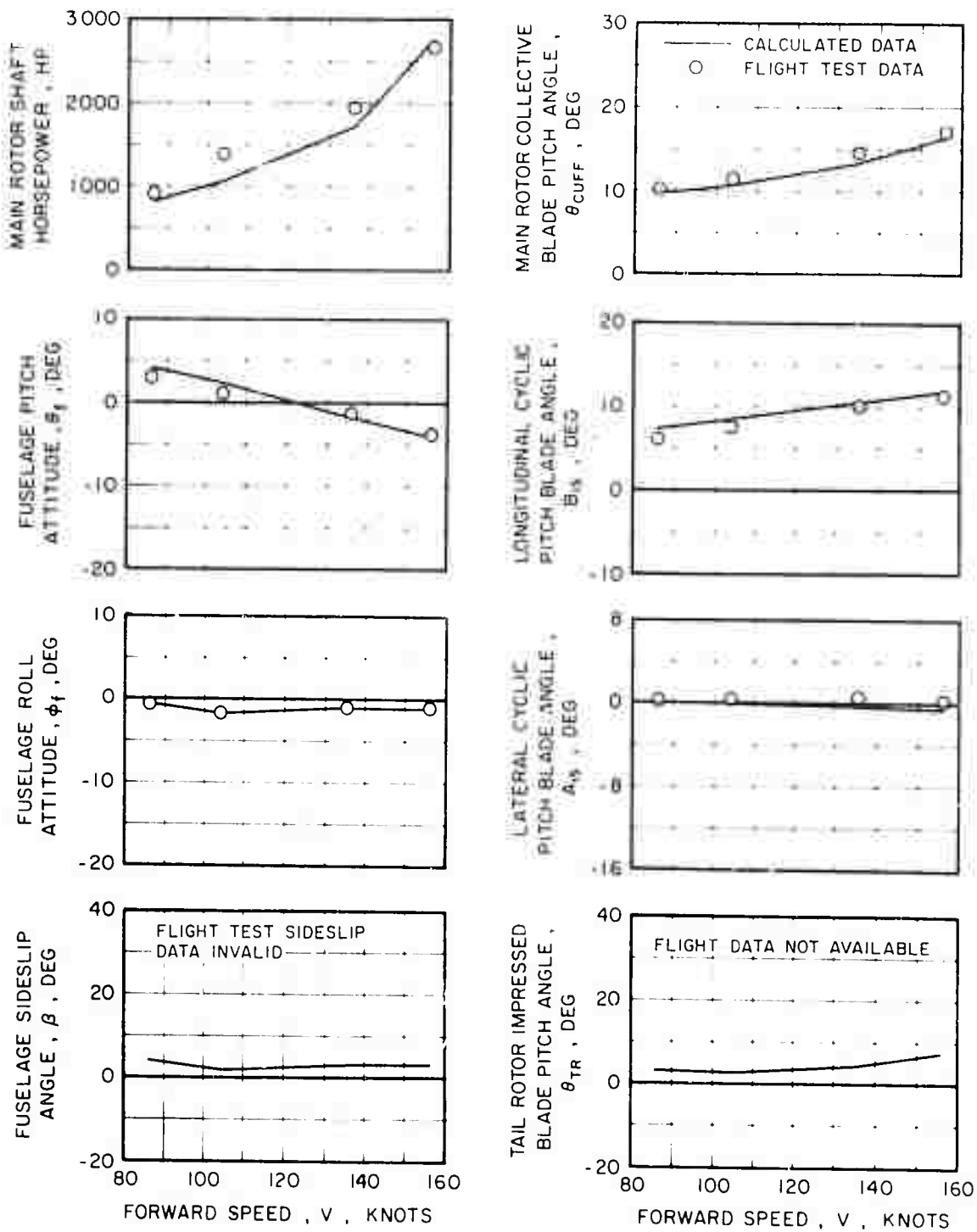


Figure 27. Comparison Between Simulated and Flight Test Data,
Level Flight Trim, GW = 14,500 lb, cg = 275 in.,
Stabilator Bias = 0 deg, Speed Brakes Extended.

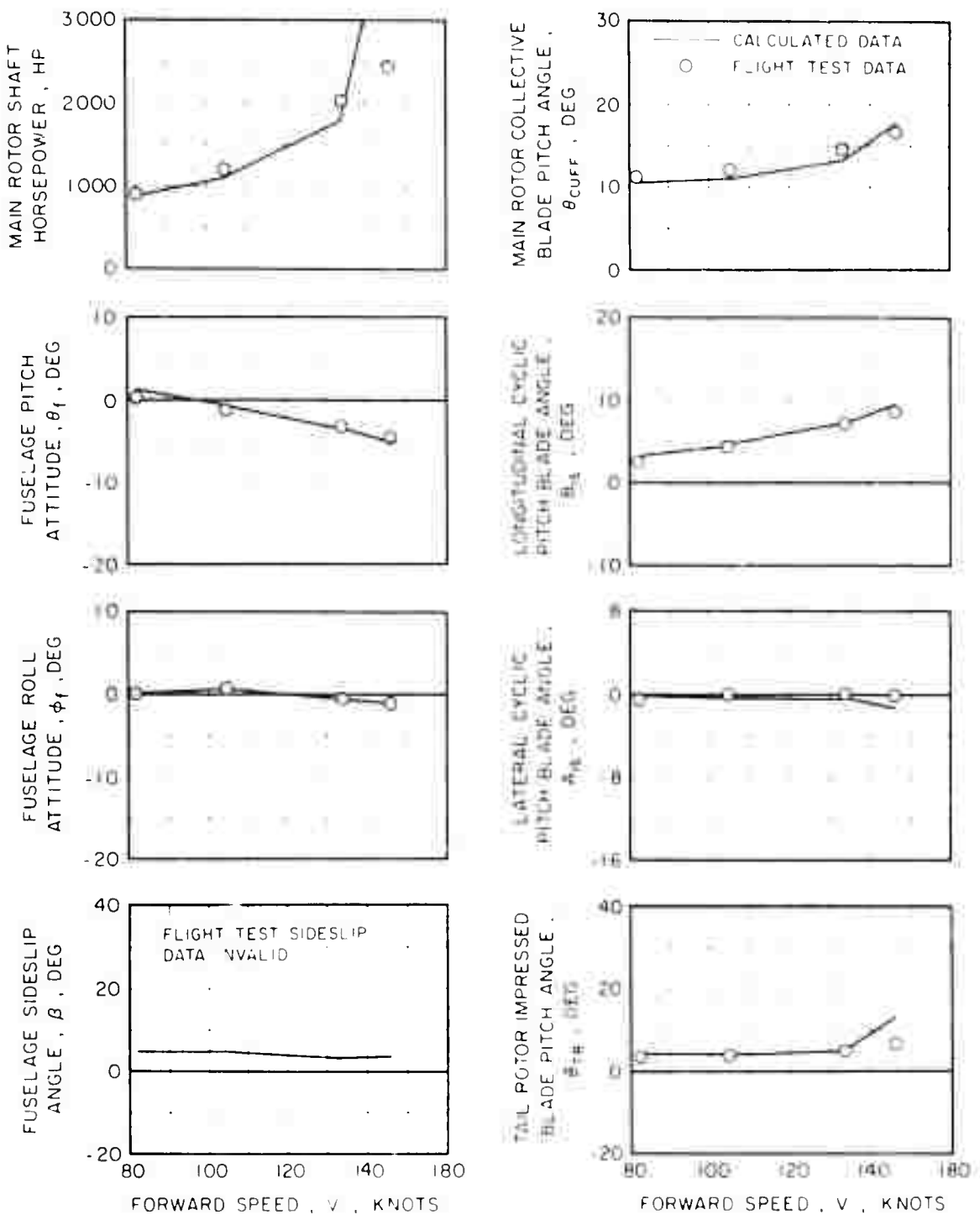


Figure 28. Comparison between calculated and flight test data, level flight trim, $W = 16,600 \text{ lb}$, $r_e = 1.4 \text{ ft}$, stabilator flap = -10° deg, speedbrake extended.

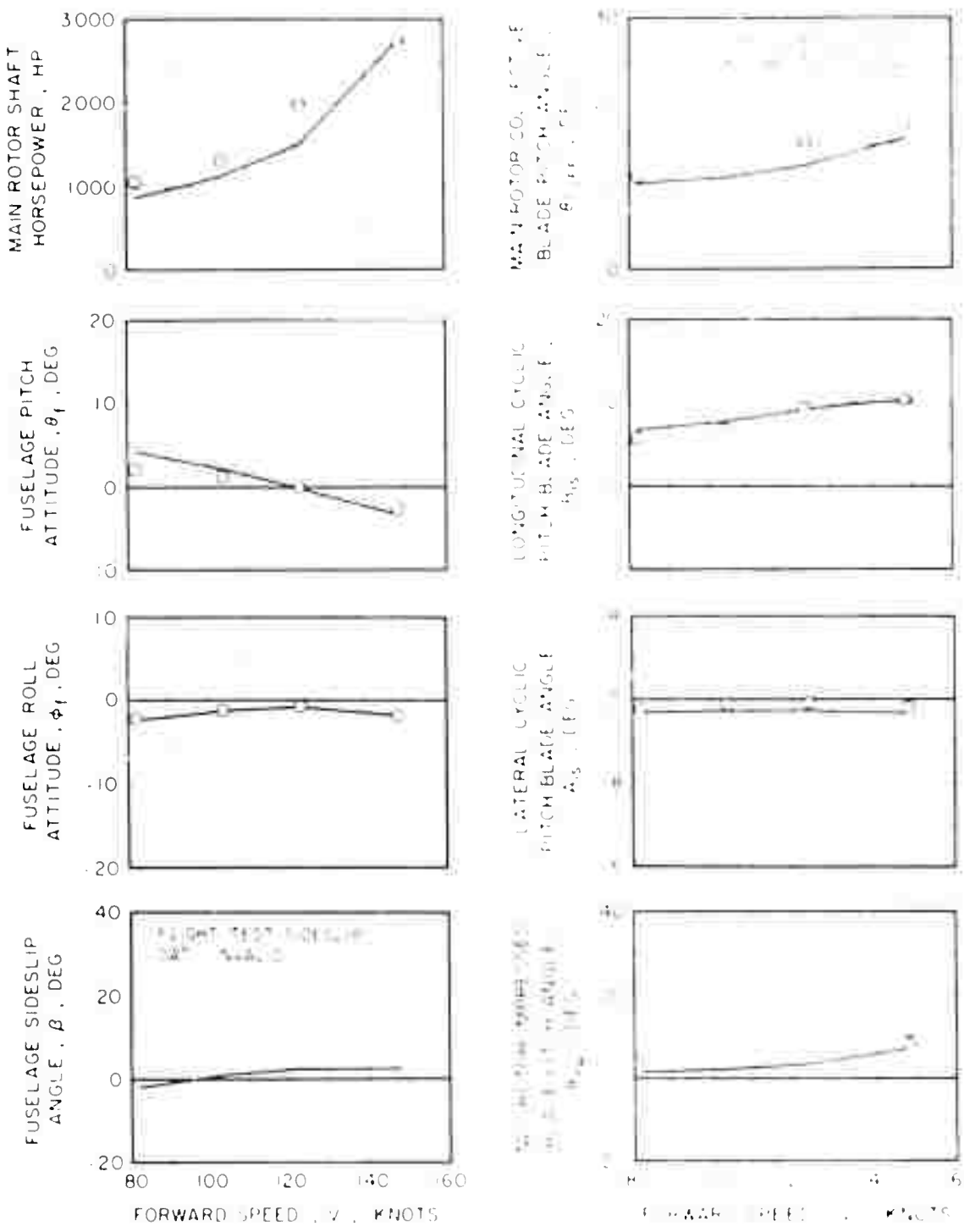


Figure 29. Control inputs and performance characteristics of the model helicopter in forward flight.